International Journal of Fatigue 154 (2022) 106556

Contents lists available at ScienceDirect

International Journal of Fatigue

journal homepage: www.elsevier.com/locate/ijfatigue

A review of fatigue damage detection and measurement techniques

Fredrik Bjørheim, Sudath C. Siriwardane, Dimitrios Pavlou *

University of Stavanger, Department of Mechanical and Structural Engineering and Materials Science, Stavanger N-4036, Norway

ARTICLE INFO

Keywords:
Fatigue
Damage
Measurement
NDT
Diagnostics

ABSTRACT

A vast amount of research has been carried out towards the goal of quantifying changes related to the fatigue damaging process in materials throughout the fatigue life. However, no recommended practice has been developed for the experimental measurement of fatigue damage before a macroscopic crack has been initiated. Therefore, this paper reviews the existing fatigue damage detection and measurement techniques on the basis of both momentum within the research field and their being considered non-destructive. The techniques are separated into two categories, namely, fatigue crack monitoring and fatigue damage monitoring. The parameters of these techniques, which quantify the physical and mechanical changes of the materials during the fatigue life, were critically reviewed in regard to the mechanism behind the change, limitations, shortcomings, etc. The acoustic emission, hardness, ultrasonic, magnetic and potential drop methods are applicable for in-situ measurements while positron annihilation and X-ray diffraction are more suitable for laboratory assessments. Even though all the revived methods are applicable for metals, acoustic emissions, X-ray diffraction, ultrasonic, strain-based and thermometric methods are also suitable for composites. The reliability, advantages, weaknesses, case/material dependency and applicability of each method are compared and tabulated for making a framework for choosing suitable technique for fatigue crack or damage detection of material or components.

1. Introduction

The iterative deterioration caused by the cyclic loading of a component or material, which eventually leads to crack initiation and, shortly after, final fracture, is generally known as “fatigue” by practising engineers. The current methodology to prevent this catastrophic failure is commonly based upon statistical analysis, with the addition of a damage accumulation rule, which is known to introduce further scatter. Furthermore, it can be seen in DNVGL-RP [1] and in a paper by Keprate and Ratnayake [2] that the common methodology for life extension involves estimating crack growth through statistical analysis and initiating an inspection program. The intervals of such an inspection program must be short enough for a detectable crack to not reach a critical size between inspections, to ensure safety during the life extension period. Consequently, the methodology in itself is fairly conservative, as the formation of a crack is certainly the simplest yet strongest indication of fatigue damage. However, the issue comes down to the fact that the crack propagation phase is commonly short, compared to the total fatigue life [3]. This results in a frequent and costly inspection program being initiated, from the time that conservative estimations of the fatigue life have been surpassed, until the point of decommissioning or, alternatively, retrofitting.

Fatigue occurs as a result of localized microstructural deformations due to cyclic loading, where the density of dislocations produced is significantly higher than for monotonic loading. The dislocations will under continued cycling form dislocation structures, such as well-defined cell structures and eventually persistent slip bands. Thereafter, microcrack initiation, coalescence and macroscopic crack propagation occurs [4,5]. Therefore, crack initiation remains the only sound methodology for assessing the remaining fatigue life, as it arises from the characteristics of the fatigue phenomenon [6,7]. This from the perspective that, detecting, measuring and assessing the fatigue damage prior to macroscopic crack initiation is quite challenging, due to the inherent nature of the phenomenon. However, the mechanisms before crack initiation will for example increase the surface hardness, generate heat, and nonuniformly deform the surface crystals, consequently resulting in the hardness-based, thermometric and X-ray diffraction methods which will be reviewed.

Regardless of the difficulties related to detecting and quantifying the accumulated fatigue damage, a vast number of researchers have performed experimental work and found several indicators of fatigue damage [8]. These indicators have contributed to the perspectives of

* Corresponding author.
E-mail address: dimitrios.g.pavlou@uis.no (D. Pavlou).

https://doi.org/10.1016/j.ijfatigue.2021.106556
Received 14 June 2021; Received in revised form 8 September 2021; Accepted 19 September 2021
Available online 22 September 2021

both better understanding the fatigue phenomenon and better predicting the remaining fatigue capacity. Even though much research has been performed, with varying degrees of success, a common practice/method/indicator has yet to be established for quantifying the accumulated damage prior to macroscopic crack initiation. Therefore, it is essential to critically review these methods from the viewpoint of accuracy, limitations, advantages, disadvantages, applicability, etc.

The objectives of this paper are to discuss the non-destructive quantifiable changes in material physical and mechanical properties throughout the fatigue life and to review the relevant detection and measurement techniques. Hence, most reliable parameters and methods are identified for investigating the related research/knowledge gaps which indicate the direction for future research.

2. Damage evaluation parameters/methods

A number of both mechanical parameters and physical measures have been proposed to be correlated with the microstructural change throughout the fatigue damaging process. The methods listed in Table 1 are chosen on the basis of both momentum within the research field and their being considered non-destructive. Momentum within the research field, is herein considered as that a number of articles from different research groups have been published regarding the method/phenomenon. The perspective of the method/phenomenon being non-destructive and having a relation to the damaging process was also considered. Furthermore, the methodologies are separated into two categories, namely, fatigue crack monitoring and fatigue damage monitoring. Fatigue crack monitoring is here considered to be the methodologies applicable after a crack has initiated, whereas fatigue damage monitoring is considered to be the phase before the aforementioned stage.

3. Crack monitoring

3.1. The potential drop method

The potential drop method (PDM) is an electric method, based on sending an electric current through the material or component and measuring the subsequent potentials at specific locations in relation to a crack. It is commonly used to either continuously or instantaneously monitor a crack in a conductive material. The methodology is based upon the fact that a crack which disrupts the continuous conductive material will significantly change the electrical potential field within the component. Therefore, crack propagation can be monitored by developing calibration curves for various crack scenarios [9]. Regarding the methodology, one can commonly discuss DC-PDM and AC-PDM; DC-PDM is the most commonly used method, whereas AC-PDM, with a high frequency current, has been observed to be more sensitive to surface cracks, due to the "skin effect" [10]. When it comes to defining calibration curves, one commonly talks about analytic, empirical and numerical methods. Gandossi et al. [11] demonstrated that finite element modelling can be used as a numerical method to develop the calibration curve with good accuracy. Spitas et al. [12] investigated the application of PDM during mixed-mode cracking, demonstrating that the application of a third sensing electrode, in contrast to the commonly used two, would result in the ability to estimate the crack angle. An example of the phenomenon can be seen in Fig. 1, developed through numerical methods, to display how the potential field is affected by the crack. Additionally, the direct current electric potential method (DC-EPM) has been considered in regard to the case of multiple small internal cracks, caused under creep-fatigue conditions, as can be seen, for example, in a paper by Tada et al. [13], which concluded that the accumulated damage could be measurable at about half the lifetime, given that the voltmeter used can measure a change of 1 percent in the potential difference.

Some examples of the accuracy of the methodology and practical examples might be such as a paper by Sonsino [14], where he compared various design concepts for the structural durability assessment of welded offshore K-nodes. In fact, the DC-PDM was adapted to define fatigue life to the initiation of a crack with a depth of about 1 mm. First detectable crack under laboratory conditions was 0.5 mm, whereas 1.0 mm for practical conditions. In [15] Černý also performed experiments on full-scale models, while monitoring the crack initiation and growth with the DC-PDM method, at elevated temperatures, also specifying that the precision of the crack length was within ±1 mm. Oppermann et al. considered in [16] the possibility of adapting DC-PDM as a means to evaluate weld seams in pipework, as a permanent installation, to reduce radiation exposure during inspection of nuclear powerplants. Herein, the perspective of achievable accuracies in monitoring is deeply discussed, from the perspective of initial length of the crack, initial crack depth and the wall thickness and length between measuring probes will affect the detectability.

Table 1
Quantifiable parameters and methods.

Category	Chapter	Method/phenomenon
Fatigue crack monitoring	3.1	Potential drop method
	3.2	Acoustic emission technique
	3.3	Ultrasonic methods
Fatigue damage monitoring	4.1	Electric resistance
	4.2	Hardness-based method
	4.3	X-ray diffraction method
	4.4	Thermometric
	4.5	Strain-based
	4.6	Positron annihilation
	4.7	Magnetic methods
	4.8	Ultrasonic methods

3.2. Acoustic emission technique

Acoustic emission (AE) is a non-destructive evaluation (NDE) method which has recently received increasing attention. The method is based on measuring the elastic stress waves, which are generated due to the rapid release of energy from a localized source within a stressed material. Thus, it is a passive methodology of NDE. Some examples of generators of elastic stress waves are plastic deformation, creep, fatigue crack nucleation and propagation, fracture and decohesion of inclusions [17,18]. It should be highlighted, however, that there are also unwanted sources of AE, such as grating between fracture surfaces, rubbing and fretting of moving parts, hammering, vibrating, rain and wind [19]. The issue of unwanted AE sources results in the application of signal

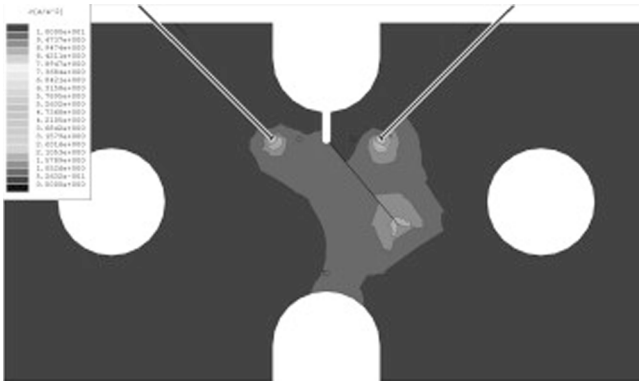

Fig. 1. Numerical methodology to develop the constant current density contours for specimen with 6.0-mm crack at 40° [12]. (Reprinted from Measurement, Volume 43, Issue 7, V. Spitas, C. Spitas, P. Michelis, A three-point electrical potential difference method for in situ monitoring of propagating mixed-mode cracks at high temperature, Pages 950–959, Copyright 2010, with permission from Elsevier.)

processing, which can be seen in works such as [20–22].

When it comes to the AE signal, it can commonly be characterized as having features such as those shown in Table 2 [20], where it can be noted that the parameters are in regard to a threshold crossing. The threshold is commonly set as a means to remove noise, by only monitoring or recording signals which exceed a certain acoustic pressure level (in dB), which in turn already highlights a weakness in the AE method. Consequently, setting the threshold too low will result in a lot of noise which is not related to the damaging process, while setting it too high might result in neglecting important signals. Thus, the threshold must be set at the "correct" level, which again is case-dependent.

As previously mentioned, the AE methodology has the advantage of being a passive method, in which the sensors detect elastic stress waves. This results both in it being applicable for continuous structural health monitoring (SHM) and that a complete scanning of the structure is not required: only a suitable number of sensors to detect the generated signals is necessary. An example of the number of sensors can be seen, for example, in [23], where it was estimated that 28 sensors were adequate to detect damage, whereas 72 would be required for damage localization for a 45.7-m-long wind turbine blade.

The AE methodology has also been investigated as a means to predict remaining fatigue life and crack extension. This can be seen in the work of Berkovits and Fang [24], who concluded that AE is an excellent tool to define initiation, and that the stress intensity factor threshold can be determined through AE, with comparable results. Furthermore, they argued that although the methodology might be complicated for estimating crack propagation, they were open to the possibility of doing so through parametric discrimination during postprocessing. Work in respect of estimating crack propagation through the use of AE signals can be seen in research by, for instance, Roberts and Talebzadeh [17,25], where an empirical relation between acoustic emission count rate and crack propagation was used. The tests were performed by extracting the count rate for the upper 5% and 10% of the applied load, with the experimental work revealing a close correlation. Similar work was also performed by Yu et al. in [26], where AE data below 80% of the peak load was removed from the dataset, and crack extension and fatigue life prediction were performed on the basis of count rate and absolute energy rate. Also to be mentioned is the study of Keshtgar and Modarres [27], who performed similar work, but using the top 40% of the peak load. All the aforementioned models on count rate and absolute energy rate follow Eq. (1):

$$\log\left(\frac{dA}{dN}\right) = B\log(\Delta K) + \log(C) \tag{1}$$

where parameter (dA/dN) is count rate, absolute energy rate or, alternatively, crack growth rate from Paris law, whereas B and C are empirical constants, depending on the methodology being used. An example of crack propagation monitoring through AE can be seen in Fig. 2, comparing the relations da/dN, dη/dN and dU/dN, being crack growth rate, count rate and absolute energy rate, respectively.

The experimental application of AE in the field can be found in, for example, detecting defects in vessels and offshore structures [18], SHM of bridges [19,28–30], wind turbine blades [23] and rail tracks [31,32], to mention a few.

Table 2
Definitions of AE time features [20].

AE Time Features	Definition
Amplitude	Peak voltage of the AE waveform
Counts	Number of threshold crossings
Duration	Time difference between the first and the last threshold crossings
Energy	Integral of the rectified voltage signal over the duration
Risetime	Time difference between the first threshold crossing and peak voltage
Counts to peak	Number of threshold crossings from first threshold to peak
Absolute energy	Integral of the square voltage signal divided by the reference resistance over the entire duration

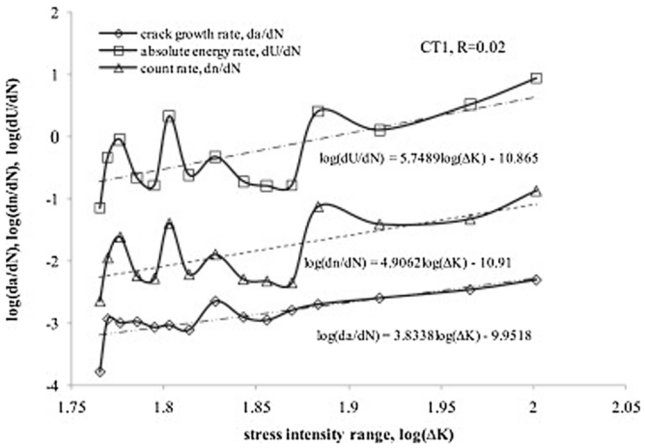

Fig. 2. Tests and regression for a CT specimen regarding the relation between da/dN, dη/dN and dU/dN, being crack growth rate, count rate and absolute energy rate, respectively, with the stress intensity range ΔK [26]. (Reprinted from Journal of Constructional Steel Research, Volume 67, Issue 8, Jianguo Yu, Paul Ziehl, Boris Zárate, Juan Caicedo, Prediction of fatigue crack growth in steel bridge components using acoustic emission, Pages 1254–1260, Copyright 2011, with permission from Elsevier.)

3.3. Ultrasonic method

The ultrasonic method is based upon sending ultrasonic waves into the material or component which is being tested, also called ultrasonic testing (UT). The ultrasonic wave is commonly generated by the use of piezoelectric transducers, whereas the non-contact technique of adapting electro-magnetic acoustic transducers (EMAT) should also be noted. As an ultrasonic wave propagate through the specimen, it will interact with discontinuities, such as cracks, which will reflect, or alternatively diffract the signal at the crack tips. Consequently, resulting in that the location and size of the crack can be determined through the sound velocity in the material and time [33].

The methods of pulse-echo and through transmission are commonly discussed in ultrasonic testing. The pulse-echo technique can be performed with either one or more ultrasonic probes, with access to one side of the part being tested. In fact, it is commonly performed by the use of an ultrasonic probe, emitting a short signal, for then to measure the subsequently reflected signal. The reflected signal will be the reflection originating from the backwall, with the addition of the signal reflected from the defect, if present. Furthermore, the intensity and arrival time of each signal will also be displayed. Consequently, resulting in that the depth to the defect, size and thickness of the specimen can be found. The through transmission technique requires both a transmitter and a receiver, with the addition of access to both sides of the specimen being tested. The transmitter will transmit a signal on one side of the specimen, which will be received by the receiver, located at the other side. If a crack or other defect is present within the scanned volume, the received signal will exhibit a lower intensity. However, the technique does not have the possibility to estimate the depth from the surface to the defect [34,35].

There are various techniques to size defects through the application of ultrasonics. Two examples might be such as the amplitude of the reflected signal from a flaw, or the time related technique of time-of-flight-diffraction (TOFD). However, it is generally accepted that the TOFD methodology is both easier to apply and more robust than the amplitude-based techniques. This from the perspective that the amplitude-based techniques commonly depend upon test pieces with

known reflectors. The test pieces should match the investigated specimen when it comes to such as material, surface finish, attenuation size and coupling conditions. Consequently, making the technique time-consuming and prone to failure if there is any difference in the reference setup and test setup. Whereas the TOFD technique is based upon the wave velocity and the diffracted signal to locate the crack tip. However, with the drawbacks of the fact that the diffracted signal will be weaker, reducing sensitivity, and that if the crack has a near surface crack-tip, the diffracted signal might coincide with the lateral signal in a commonly used pitch-catch configuration [36,37].

Examples of what has been done in regard to the TOFD technique might be such as Nath et al. who reported the possibility of sizing cracks from the outer surface in solid steam rotor shafts in [38] by the manual ultrasonic TOFD technique. Subsequently, they developed experimental probability of detection (POD) and probability of sizing (POS) curves for the complex geometry in [39]. Habibpour-Ledari and Honarvar discussed in [40] the weakness of TOFD being a two-dimensional technique. Subsequently proposing a method to locate and size defects in three dimensions, through the use of more transmitters and receivers with theoretical methods currently being used in radar systems. In fact, two algorithms were tested and compared, showing promising results. In [41] Chang and Hsieh proposed a double-probe TOFD imaging method to detect nonhorizontal flaws which could not be detected by the use of the common pulse-echo technique. Baskaran et al. Proposed in [35] the shear-wave time-of-flight-diffraction (S-TOFD) with the objective of achieving higher accuracy during near-surface inspection. Furthermore, the signal processing technique called Embedded Signal Identification Technique (ESIT) [42] was adapted to further increase accuracy. It was found that an EDM notch of 0.5 mm was sized to 0.52 mm through the combined method of S-TOFD and ESIT. Furthermore, for a fatigue crack of 2.63 mm, the application of S-TOFD alone sized it to 2.57, whereas the combination of S-TOFD and ESIT resulted in a sizing of 2.64 mm. Subbaratnam et al. highlights the limitation of TOFD for thinner sections [43]. Subsequently, proposing a technique of immersion TOFD for thin sections. This is from the perspective that immersion helps to provide sufficient time delay. The investigated material had a thickness of 3 mm, with artificial flaws down to 0.09 mm depth which were measured with good accuracy.

In [44] Masserey and Fromme investigated the application of high frequency guided waves to monitor the development of fatigue cracks at fastener holes in aircrafts. Concluding that a fatigue crack of 0.8 mm^2, which corresponded to about 1 mm depth could reliably be detected. Another study regarding sensitivity for the ultrasonic methods has been reported by Grubisic and Sonsino [45]. Crack initiation was detected by continuous ultrasonic measurements with several fixed 45°-US-sender/receivers; under laboratory conditions first detectable crack depth a = 0.25 mm, whereas under practical conditions a = 0.5 mm.

4. Damage monitoring

4.1. Electric resistance

The methodology for damage monitoring through electrical measurements has the same fundamental application as the methodology for crack monitoring. However, the parameter for damage monitoring is the change in resistance. The argument for the increased resistivity comes from cases such as dislocations, point defects, micro and macroscopic crack propagation [46]. However, there are other factors which might also affect the resistivity of the specimen, such as elongation, temperature or reduction of cross section, resulting in the fact that other changes which can influence the measurement must be eliminated or accounted for [47]. Starke et al. demonstrated how the resistivity can be used as a means to reveal initial material condition within a group of specimens made from the same material in [48], as can be seen in Fig. 3. Consequently, as the initial resistivity and the number of cycles to failure were in good correlation, higher initial resistance was attributed to a higher number of initial defects. Furthermore, it was demonstrated that resistivity can be applied to estimate the stress amplitude at the knee-point of the Woehler-line through a load increase test (LIT). Germann et al. applied resistance monitoring during common fatigue tests of three different steels in [49], revealing that the materials would exhibit an initial reduction in resistance, before then having a sharp increase towards failure. Both the maximum decrease and the following maximum resistance depend upon the applied stress amplitude. The initial reduction of resistance was also investigated through the application of scanning electron microscopy (SEM), revealing that the cause was closure of microcracks. Mao et al. proposed and demonstrated a method for damage detection and damage localization in [50], through the use

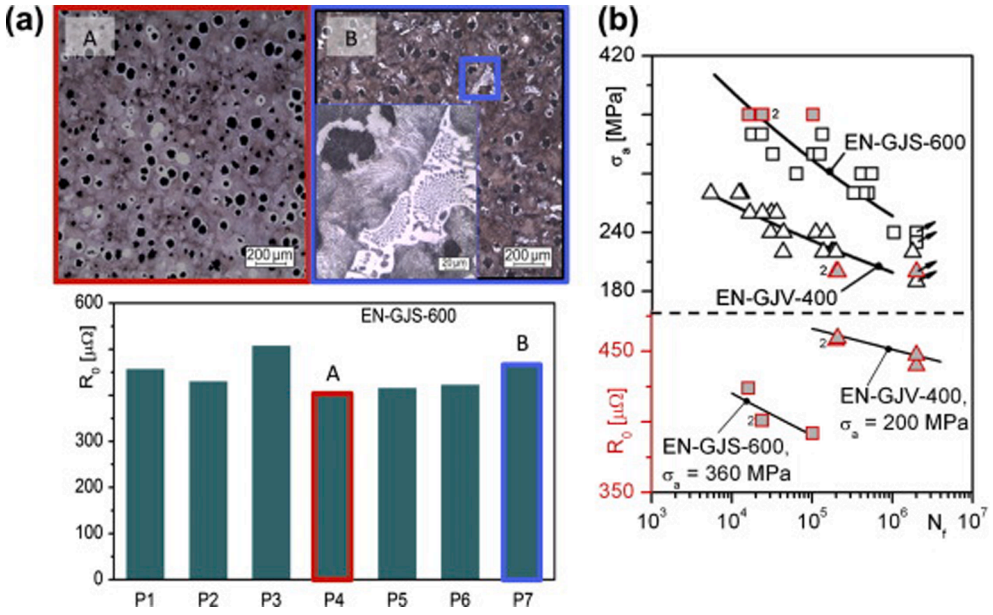

Fig. 3. Initial resistivity with the respective microstructures for cast iron EN-GJS-600 (ASTM 80-55-06) (a) and S-N curves, as well as initial resistivity-lifetime relation for EN-GJV-400 and EN-GJS-600 (ASTM 80-55-06) (b) [48]. (Reprinted from International Journal of Fatigue, Volume 82, Part 2, P. Starke, D. Eifler, C. Boller, Fatigue assessment of metallic materials beyond strain measurement, Pages 274–279, Copyright 2015, with permission from Elsevier.)

of a suitable number of electrodes and the application of an equipotential lines back-projection algorithm. However, the drawback is that accuracy is a function of measurement electrodes used. Klein and Eifler investigated the fatigue strength of different manufacturing processes, through the application of simultaneous measurements of temperature, resistivity and plastic strain amplitude, demonstrating that the change in both resistance and temperature is a better early warning sign, compared to plastic strain [51].

The parameter of resistivity has also resulted in the development of an accumulative damage model by Sun et al. [47,52]. However, it was not checked for variable amplitude loading. Furthermore, it could be seen that this material did not exhibit an initial decrease in the resistance, in contrast to the aforementioned research, highlighting the material dependence of the resistance method. Several other studies have also been performed, reporting similar results [53–57].

4.2. Hardness-based method

The argument for using hardness measurements as a means to evaluate fatigue damage originates from the crack initiation stage, commonly discussed as a surface phenomenon which is due to microplasticity at the free surface.

An early study of the correlation of fatigue damage with changes in the surface hardness can be found in [58]. In this work, there is experimental evidence that the fatigue damage accumulation until crack initiation can be reflected by changes in the surface Vickers hardness for aluminium specimens. In 2002, these findings were utilized to derive a nonlinear fatigue damage accumulation rule of the damage function D versus the stress amplitude and number of loading cycles [59]. The proposed model was verified in two-stage variable loading experimental results, showing very good accuracy.

Correlation of hardness change with the fatigue damage has also been carried out by Ye et al. [60,61], who worked on the microhardness level with a Vickers indentation, revealing that the statistical mean of the microhardness for both ferrite and pearlite would change throughout the fatigue life. In fact, both phases would display an initial hardening, stabilizing and then decreasing until failure, as can be seen in Fig. 4, including the full range of scatter bars. Furthermore, Ye and Wang argued [62] that the hardness measurement is a stochastic variable, then concluded that the damage variable should be a probabilistic

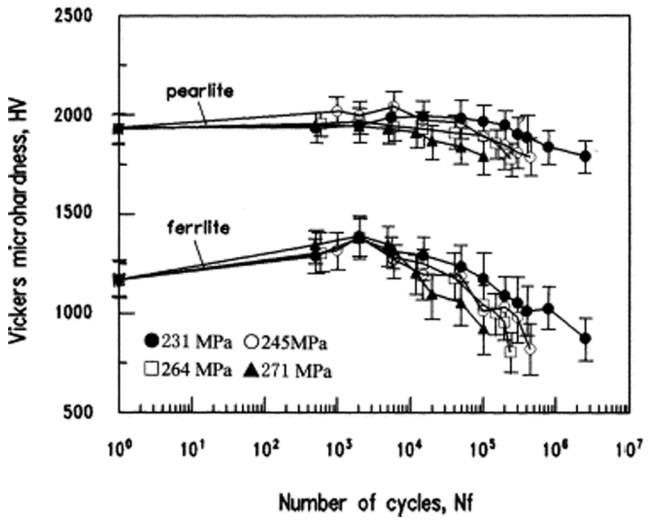

Fig. 4. Change and error bars with the total range of microhardness in ferrite and pearlite during fatigue loading [62]. (Reprinted from International Journal of Fatigue, Volume 23, Issue 1, Duyi Ye, Zhenlin Wang, An approach to investigate pre-nucleation fatigue damage of cyclically loaded metals using Vickers microhardness tests, Pages 85–91, Copyright 2001, with permission from Elsevier.)

function, subsequently adapting the normal distribution function to represent the probabilistic accumulated damage throughout the fatigue life.

Drumond et al. [63–65] investigated the microhardness evolution in API 5L X65 for both annealed and as-received specimens throughout the fatigue life, by the use of a Berkovich indentation. The findings were that, early in the fatigue life, the annealed specimens would initially harden, then soften, whereas the specimens in the as-received state would initially soften, then harden, highlighting the important role of initial material condition, as in dislocation structure. Furthermore, the results show that the change is certainly more prominent at the surface, as indentation depths of 2, 4 and 6 μm were measured, with the most significant change in hardness being observed for the 2 μm measurements.

Additionally, Miroslav et al. [66] investigated the microhardness evolution, through the use of Vickers indentations, and the hardness evolution, through Brinell of a S355J0 steel, which also followed the aforementioned described change. This highlights the applicability of Brinell measurements, which do not require the same level of surface preparations as in the case of the aforementioned Vickers microhardness test. Furthermore, the perspective of what qualifies as a good diagnostic method for the changes in the mechanical properties of the surface material was discussed, in which it was stated that the diagnostic method should:

- Be simple, and allow for use in operational conditions
- Target the surface layer of the material
- Have minimal influence on the material

In light of this, it should be mentioned that the methodology of hardness evolution throughout the fatigue life might be fairly applicable in regard to the understanding of the accumulated fatigue damage. However, its application as a diagnostic tool for in situ measurements might be questionable. This comes from the perspective that the fatigue phenomenon is known to be sensitive regarding notches or other discontinuities of material that cause stress concentrations, consequentially resulting in the fact that hardness measurements might not be a non-destructive method. The microhardness methodology might be more applicable in respect of the fact that it is a less intrusive indentation; thus, it can be argued that it actually is non-destructive. However, it comes with another disadvantage. In fact, Ye et al. [60] specify that the prerequisites for microhardness measurements are such that the specimens must be polished by an electro-chemical method, before being etched to reveal the microstructures; this must be performed before fatigue cycling is applied, as polishing a fatigue-damaged specimen would partly, if not fully, remove the strain-hardened/softened surface grains.

4.3. X-ray diffraction method

The X-ray diffraction (XRD) methodology is commonly applied for two reasons: (a) to determine residual stresses (macro stresses), through the $\mathrm{SIN}^2\Psi$ method, or (b) to determine the dislocation density (micro deformations), through different methods of characterizing diffraction profile broadening [67]. Fig. 5 depicts the two observed changes to the peak of an XRD due to macro stresses and micro deformations, resulting in a peak shift and a peak broadening, respectively. The most common way to evaluate peak broadening is through the full width at half maximum (FWHM), due to its simplicity. However, maintaining comparable sensitivity to the integral method, with the exception of the early stages, was demonstrated by Vijayan et al. [68]. Nagao and Weiss investigated low cycle fatigue of plain carbon steel in [69] through XRD. The material had three different initial conditions: strain aged, 20% prestrained and as received, to investigate the effect of initial conditions for low cycle fatigue (LCF), concluding that after 10% of the fatigue life, the materials were independent of the initial condition. Pangborn et al. [70] investigated the dislocation density-depth profile in single crystals of

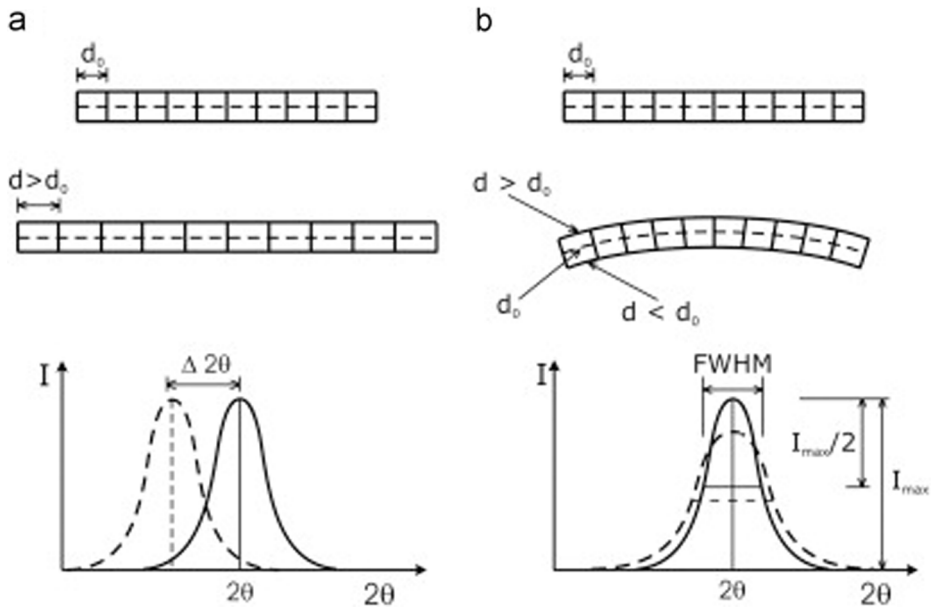

Fig. 5. Influence of (a) macro stresses (uniform deformation) and (b) micro deformations (nonuniform deformation) on X-ray diffraction peak [72]. (Reprinted from Materials Science and Engineering: A, Volume 580, B. Pinheiro, J. Lesage, I. Pasqualino, E. Bemporad, N. Benseddiq, X-ray diffraction study of microstructural changes during fatigue damage initiation in pipe steels: Role of the initial dislocation structure, Copyright 2013, with permission from Elsevier.)

aluminium, silicon, gold and polycrystalline Al-2024, after monotonically inducing a plastic strain. It was found that the dislocation distribution for monotonically loaded specimens exhibited a high number of dislocations at the surface, whereas it dropped continuously before converging towards the bulk material. However, the cyclically loaded specimens of polycrystalline aluminium, in addition, exhibited a minimum at a depth of about 100 μm, which was more marked with continued cycling. An important conclusion from the work, however, was that the three-stage sequence commonly observed in the fatigue damage evolution curve, through the use of XRD, is due to the application of low penetrating radiation, combined with early saturation of the surface. Thus, the application of deep penetrating molybdenum radiation in contrast to copper was applied, finding that the molybdenum resulted in a fairly linear increase of excess dislocation density throughout the fatigue life, subsequently demonstrating that XRD has the capability to estimate remaining fatigue life with good accuracy for a specimen previously subjected to four block loads of increasing amplitude. Kramer et al. continued this work on determining the dislocation density in depth of steels, aluminium and brass in [71]. In contrast to the findings for aluminium, the steel only exhibited a minimum in the dislocation-depth profile for the early stages of fatigue damage. In fact, the profile was similar to the monotonically loaded specimens, where

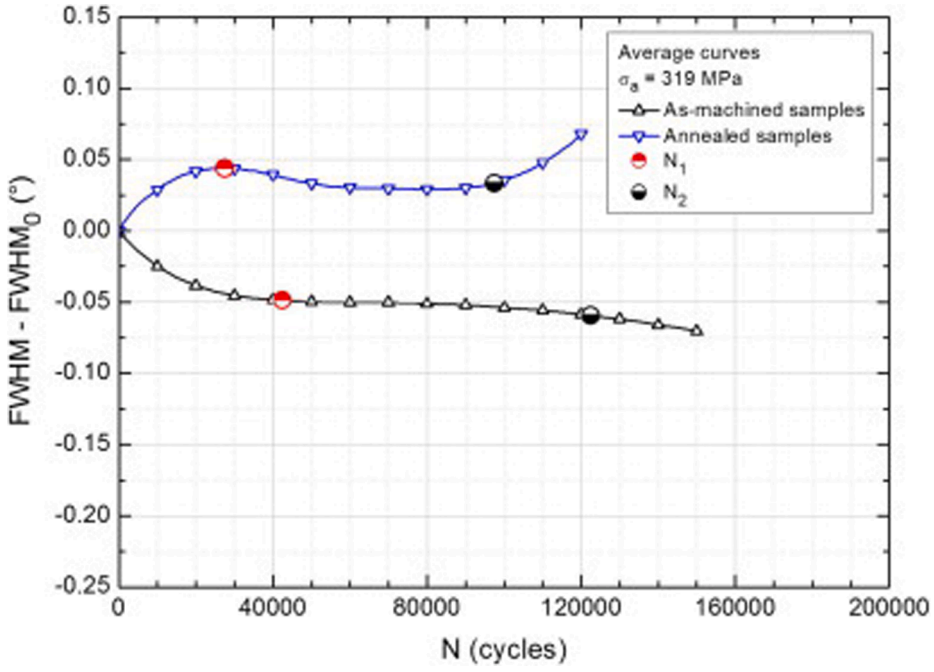

Fig. 6. Change of FWHM under fatigue cycling for as-machined and annealed samples of API 5L X60 at a stress amplitude of 319 MPa (R = −1) [72]. (Reprinted from Materials Science and Engineering: A, Volume 580, B. Pinheiro, J. Lesage, I. Pasqualino, E. Bemporad, N. Benseddiq, X-ray diffraction study of microstructural changes during fatigue damage initiation in pipe steels: Role of the initial dislocation structure, Copyright 2013, with permission from Elsevier.)

the conversion value of the bulk density increased towards the surface density with continued cycling. Pinheiro et al. [67,72] investigated pipeline steel with a ferritic-pearlitic microstructure, with the initial conditions as-machined and annealed states, under cyclic loading through the FWHM method. The radiation used was Cr-Kα radiation, which has a penetration depth of 5.8 μm for the ferritic-pearlitic steels at a tilt angle of 0, resulting in a three-stage sequence in the damage accumulation. However, the results highlight the effect of initial dislocation structure, as can be observed in Fig. 6. In fact, the as-machined specimens exhibited a reduction in peak width, whereas the annealed specimens exhibited the commonly discussed peak broadening.

4.4. Thermometric

The thermometric method is based on the absorbed hysteresis energy during fatigue cycling, where most of the energy (80–100%) is dissipated into the surroundings as heat, whereas a small portion increases the internal energy [73,74]. It is commonly agreed that a typical temperature-cycles curve will exhibit three stages, namely, increase, stabilization and failure [75,76]. When it comes to application of the thermometric methodology, a number of researchers have investigated and concluded that the energy dissipated as thermal energy can be used to determine the stress amplitude at the knee-point [77–81] and the fatigue curve [82–86], commonly based on temperature monitoring. An example of how the stress amplitude at the knee-point can be assessed in regard to thermal readings is presented in Fig. 7, where the commonly accepted stabilization temperature is exploited. In the aforementioned literature, for both the thermometric and the resistance-based methods, the knee-point is discussed as the fatigue limit or endurance limit. However, it is well documented that neither an endurance limit nor a corresponding threshold stress intensity exists [87,88]. Thus, it should be acknowledged that the knee-point stress amplitude can be found, whereas it also defines a limitation of the methodology, in regard to stress/strain amplitude domain.

Meneghetti investigated the dissipated energy in a unit volume of a material per cycle, concluding that the parameter is only dependent on load ratio and the applied stress, in contrast to surface temperature, which is also dependent on specimen geometry, test frequency and the thermal boundary conditions [89]. Boulanger et al. [90] separately identified the dissipative and thermoelastic sources, allowing the measurement of very low dissipation in comparison to the thermoelastic sources. Furthermore, the parameter of temperature is commonly very sensitive, in comparison to factors such as plastic strains. This can be seen in the aforementioned literature, where temperature and plastic strains are simultaneously monitored, but they were also explicitly mentioned by, for instance, Luong in [79] and Weber in [74]. Weber also included a practical example, in which a specimen cycled to 5×10^6 cycles at 37 Hz exhibited a temperature change of 10 Kelvin, while exhibiting a plastic strain of magnitude 10^{-4}. However, care should be taken in regard to frequency and stabilization temperature. An example of this can be seen in a paper by Liaw et al. [91], in which it was stated that the significantly higher stabilization temperature could contribute to the reduction of fatigue curves developed by 1000 Hz, in comparison to 20-Hz cycling.

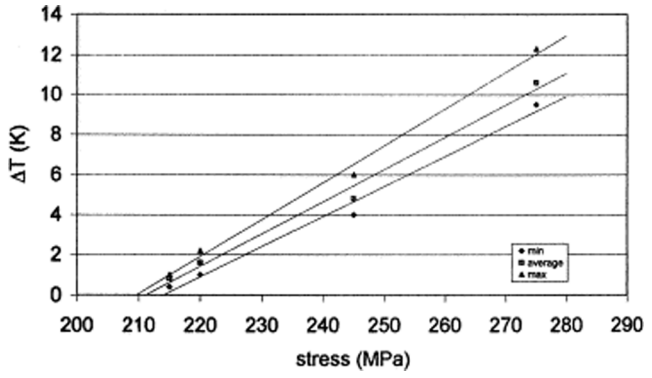

Fig. 7. Knee-point estimation through the use of the stabilization temperature [77]. (Reprinted from International Journal of Fatigue, Volume 22, Issue 1, G La Rosa, A Risitano, Thermographic methodology for rapid determination of the fatigue limit of materials and mechanical components, Pages 65–73, Copyright 1999, with permission from Elsevier.)

Furthermore, Amiri and Khonsari proposed the temperature-rise angle as a good candidate for fatigue damage indicator in [92]. They measured this by inserting cool-down periods within the fatigue loading test, before then measuring the new raise angle. Liakat and Khonsari proposed a method to evaluate the remaining fatigue life of damaged material in [93], with the aforementioned raise angle parameter, subsequently verifying the methodology for a two-stage loading from low to high and high to low with reasonable accuracy. It should be highlighted, however, that the parameter has a high load condition dependence, resulting in the fact that the stress range, mean stress and frequency must be defined to monitor the raise angle.

4.5. Strain-based

The strain-based methodologies can be separated into two different categories, namely, inelastic strains and ratcheting, as can be seen in Fig. 8 and Fig. 9, respectively. Ratcheting is commonly attributed to local deformation around voids, non-metallic precipitations and other defects within the material [94–96].

Dietrich and Radziejwska investigated the damage development in a cast Al-Si-Cu alloy through strain measurements in [94]. It was found that the main mechanism for fatigue damage for this material is ratcheting, justified through the fairly constant inelastic strains, with a continuous increase in mean strain. Damage accumulation curves were developed for the material, highlighting its nonlinearity and that the marked change in the parameter is observed early in the fatigue life.

Socha investigated the inelastic strains throughout the fatigue life of a structural steel under fully reversed cyclic loading for different stress amplitudes in [97], separately identifying the three commonly discussed fatigue damage accumulation stages: (a) elastic work of undamaged material, (b) micro crack initiation and growth, followed by (c) dominating crack propagation. This ended in a proposed method for fatigue life prediction, in light of the aforementioned stages, as the sum of Miner's rule, change of inelastic strains and macroscopic crack propagation. Socha also investigated three other structural steels in [98], with the introduction of damage progress rate curves, and proposed a formula for fatigue life prediction. The validity of the formula was checked, revealing good accuracy for two-stage loading from high to low and low to high, with the exception of one of the steels exhibiting high scatter for the high to low scenario. The scatter was attributed to early formation of Lüders bands.

Furthermore, the methodology of strain measurements has been used as a means to continuously monitor for crack initiation in regard to notches. This can be seen for instance in a paper by Sonsino [99] where the effect of cold forming was investigated for the cyclically softening steel Fe E 47 and the cyclically hardening aluminium alloy AlCuMg2 under low cycle fatigue. First detectable crack depth was a = 0.25 mm.

4.6. Positron annihilation

Positron annihilation spectroscopy has its basis in sending positrons into the material and registering the subsequent annihilation. The methodology has many applications. The main concepts which are applied in regard to non-destructively investigating fatigue damage accumulation are the time for a positron to annihilate and the energy distribution between the two resulting photons, commonly discussed as positron annihilation lifetime (PALS) and line shape analysis, the latter of which might be evaluated through the S-parameter, as seen in Eq. (2).

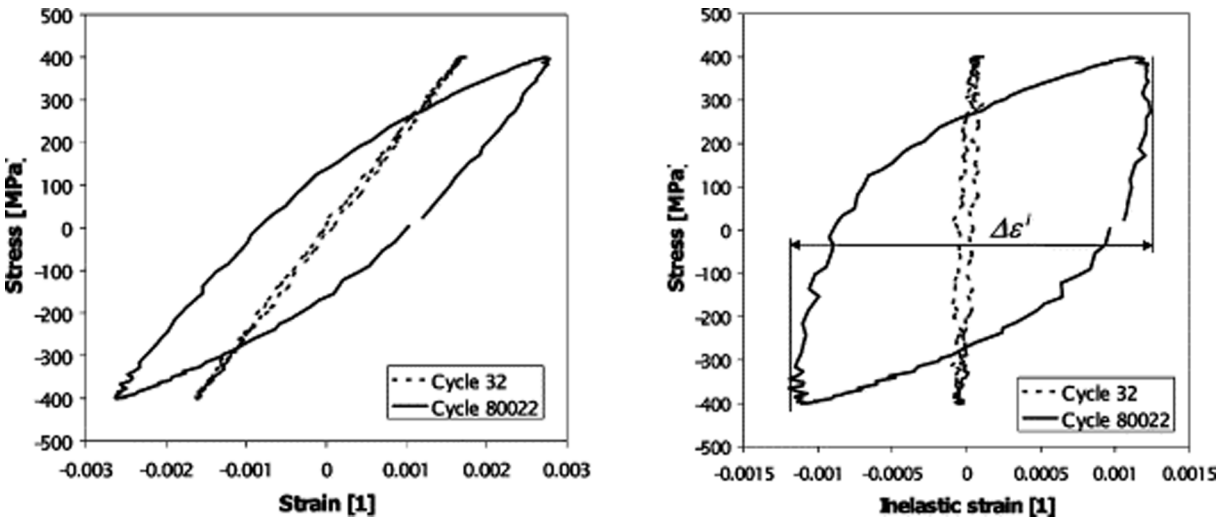

Fig. 8. Example of hysteresis loop recorded for cycle numbers 32 and 80,022 in structural steel A10, according to a Polish standard PN-73/H-84026, with a stress amplitude of 400 MPa [97]. (Reprinted from International Journal of Fatigue, Volume 25, Issue 2, G. Socha, Experimental investigations of fatigue cracks nucleation, growth and coalescence in structural steel, Pages 139–147, Copyright 2002, with permission from Elsevier.)

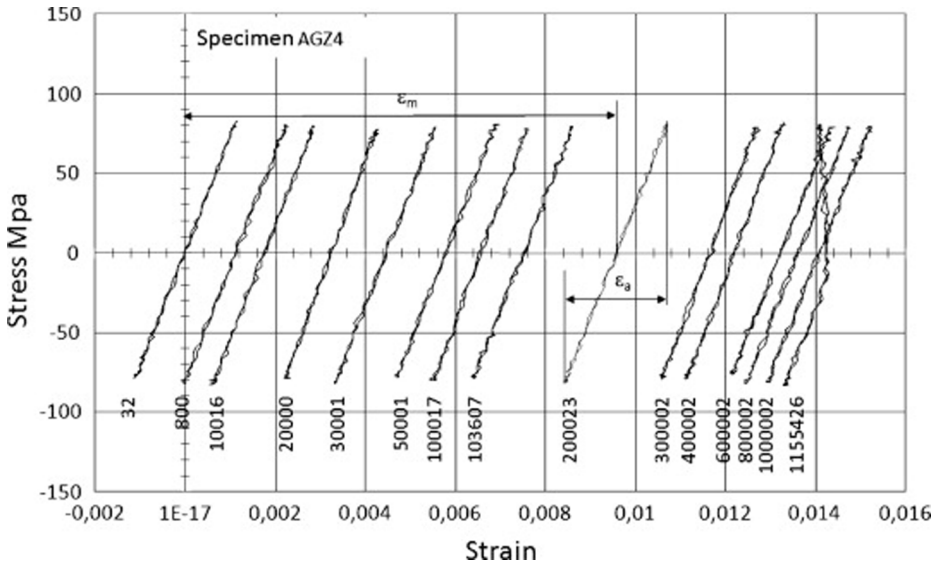

Fig. 9. The stress–strain curves of selected cycles in a cast Al-Si-Cu alloy specimen tested under stress amplitude equal to 80 MPa (The comma represents the decimal) [94]. (Reprinted from Materials & Design, Volume 32, Issue 1, Lech Dietrich, Joanna Radziejewska, The fatigue damage development in a cast Al–Si–Cu alloy, Pages 322–329, Copyright 2010, with permission from Elsevier.)

The increased time from birth to annihilation of a positron comes from the perspective that annihilation is a stochastic process, where the positron annihilation rate, or the probability of annihilation per unit time, is related to the local electron density. Furthermore, the resulting photon energy distribution comes from the fact that the positron-electron pair is not at rest, meaning that the momentum also has to be carried away by the radiation. The density and momentum of electrons commonly seen at positron trapping sites are observed to be lower, resulting in a longer lifetime and a sharper energy distribution curve. A positron trapping site is an open volume defect, such as vacancies, grain boundaries, precipitate, to mention a few [100–102]. Furthermore, a representation of the birth to annihilation for a positron can be seen in Fig. 10, both for the case of annihilation in the bulk and a positron trap.

$$\mathrm{S-parameter} = \frac{\text{The counts of } \gamma - \text{ray near central peak}}{\text{Total counts of } \gamma - \text{ray}} \quad (2)$$

Throughout the following reviewed literature, it can be seen that both dislocations and vacancies are discussed as positron trapping sites. However, in a review paper on positron annihilation spectroscopy by Čížek [101], it was discussed that the dislocations are shallow positron traps with a binding energy less than 0.1 eV. Thereafter, a generally accepted concept is mentioned of a two-step process, where the positrons at first are trapped in the dislocation core, before diffusing along the dislocation line, eventually being trapped at vacancies anchored in the elastic field of the dislocation, resulting in a slightly shorter lifetime than for a monovacancy, as the anchored vacancies will be compressed due to the elastic stress field of the dislocation. In light of this, it should also be mentioned that other researchers also highlight the development of vacancies through plastic deformation and fatigue [100,103,104].

Uematsu et al. investigated the possibility of using positron annihilation as a means of crack detection for 316 SS in [105], finding that the lifetime analysis is suitable for detecting crack initiation, whereas the line-shape analysis could not. However, it was highlighted that both parameters are capable of detecting fatigue damage, exhibiting a

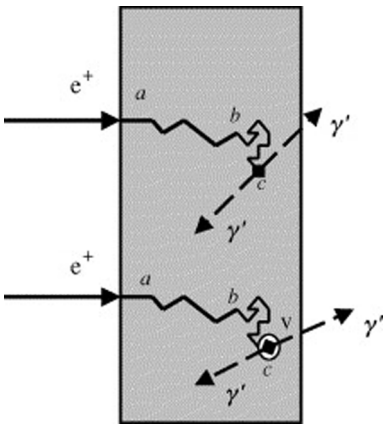

Fig. 10. Schematic view of possible fates of positrons implanted in a solid. Upper track: implantation (a), slowing-down (a to b), thermal diffusion (b to c), annihilation at c with a bulk electron and emission of two photons (γ′). Lower track: same as above from a to c, trapping at c in a vacancy (v), annihilation in v and emission of two photons (γ′) [100]. (Reprinted from Acta Materialia, Volume 52, Issue 16, A. Dupasquier, G. Kögel, A. Somoza, Studies of light alloys by positron annihilation techniques, Pages 4707–4726, Copyright 2004, with permission from Elsevier.)

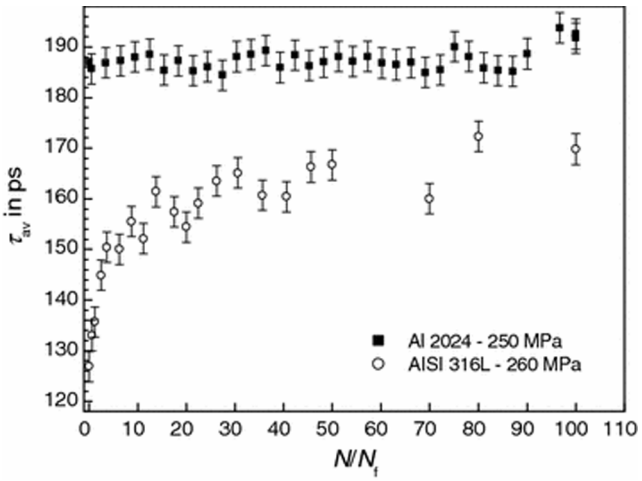

Fig. 11. Comparison of the evolution of average positron lifetime τ_{av} during stress-controlled fatigue experiments between stainless steel AISI 316 L and the aluminum alloy 2024. The number of fatigue cycles N is normalized to number at failure N_f. The error bars denote the accuracy of the positron lifetime measurement of ±3 ps [111]. (Reprinted by permission from Springer Nature, Journal of Materials Science, On the non-destructive detection of fatigue damage in industrial aluminium alloys by positron annihilation, Holzwarth, U., Schaaff, P., Copyright 2007.)

continuous increase throughout the fatigue life of the specimen.

Kawaguchi et al. investigated 316 SS for both low stress and low strain through the S-parameter, highlighting its increase throughout the fatigue life, and how the evolution depends on whether the test is stress or strain controlled [106]. Furthermore, Kawaguchi and Shirai investigated the different components of the lifetime spectra, highlighting that the lifetime of the different defect types changes little, whereas the relative intensity increases, subsequently highlighting that, in contrast to line shape analysis, the PALS has the advantage of identifying defects [107].

Although several researchers document a continuous increase in PALS and continuous sharpening of the S-parameter, it should be highlighted that the methodology sometimes exhibits saturation before fatigue failure, thus possibly being more applicable to early-stage fatigue. Examples of this can be seen in such as [108] for 316 SS, reporting a significant change in the S-parameter from 0% to 10% of the fatigue life, whereas a very small increase from 10% to 100%. Furthermore, in [104], it was reported that the positron lifetime did not exhibit significant change after 50% of the lifetime in the SS 316L. Similar studies reporting early saturation have also been performed on SS 304 [109,110].

Holzwarth and Schaaff investigated the applicability of PALS for industrial aluminium alloys, concluding that there was no significant change in the measured PALS throughout the fatigue life, attributed to the high density of precipitates which mask the accumulated fatigue damage in respect of PALS, as can be seen in Fig. 11. This essentially highlighted the importance of microstructure in regard to the methodology [111]. Furthermore, in [103], the same authors investigated AISI-316 L under both stress and strain control conditions, highlighting how the methodology is much more pronounced in the earlier stages of fatigue damage accumulation.

4.7. Magnetic methods

Within the field of magnetic methods of determining accumulated fatigue damage for ferromagnetic materials, methods such as Barkhausen noise (BHN) or magnetic hysteresis are commonly discussed. The fundamental argument for the magnetic methods is the strong relation between the magnetization process and the microstructure [112], commonly attributed to the fact that the magnetization process is through movement of the domain walls within the material, which will be affected by different microstructural characteristics [113–115]. Several studies have been performed on how the magnetic methods might be affected by such characteristics as grain boundaries [116], inclusions [117] and dislocations [118,119], amongst others [120,121]. However, in the light of fatigue damage, it is commonly the accumulated dislocation structure which is discussed.

4.7.1. Barkhausen noise

Lindgren and Lepistö investigated the application of a new sensor which could continuously monitor BHN during the fatigue life, in which the dimensional changes of the specimen took care of the magnetization (mechanical BHN) [122]. Furthermore, they investigated the fatigue of a mild steel specimen which was loaded in bending, while investigating the BHN in different directions in comparison to the commonly used loading direction. They concluded that measuring BHN in only one direction might result in misevaluation of the fatigue damage. In fact, the most prominent changes observed were at approximately a 45° angle, as presented in Fig. 12 [123].

Soultan et al. also investigated the mechanical BHN in iron specimens in [124], finding that the root mean square (RMS) of the mechanical BHN is load frequency dependent and would not have an initial increase for stress amplitudes beneath the fatigue knee-point stress amplitude. Furthermore, it was noted that the variation in BHN throughout the fatigue life could be divided into three stages, namely, a transient stage, a stationary stage and a reduction, ending in fracture. The observed stationary stage linearly increased with applied stress amplitude up to the fatigue knee-point stress amplitude, whereas it started to saturate as the stress amplitude exceeded the knee-point stress amplitude of the material.

Palma et al. investigated the magnetic BHN of AISI 8620, a ferritic pearlitic steel, subjected to rotating bending fatigue, and axially loaded with R = 0 [125]. They found that no change was observed with amplitudes beneath the knee-point stress amplitude, whereas small changes could be observed slightly above this knee-point stress amplitude. Furthermore, the parameter was more marked with higher amplitude loading, whereas it was significantly reduced in axial testing if the maximum stress surpassed yielding, as observed in Fig. 13. Thus, they concluded that the methodology was not applicable for stresses above the yield limit.

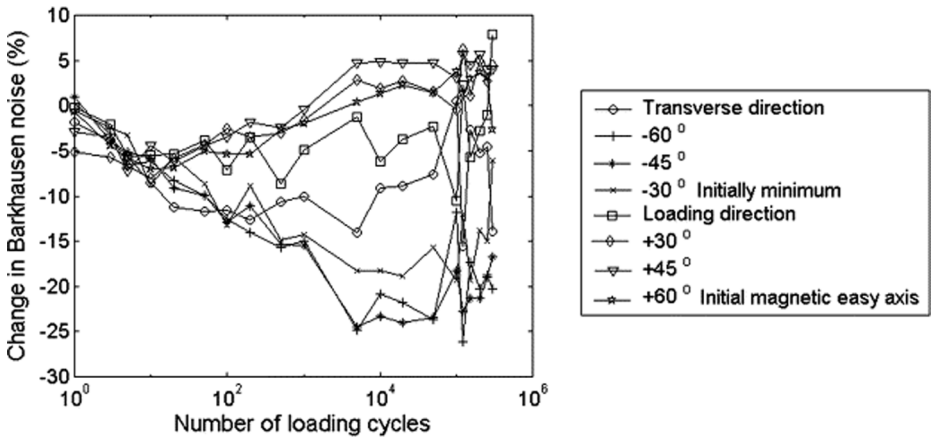

Fig. 12. Change in Barkhausen noise in different measuring directions through the fatigue life with a strain amplitude of 1000 μ Strain [123]. (Reprinted from NDT & E International, Volume 36, Issue 6, M. Lindgren, T. Lepistö, Effect of cyclic deformation on Barkhausen noise in a mild steel, Pages 401–409, Copyright 2003, with permission from Elsevier.)

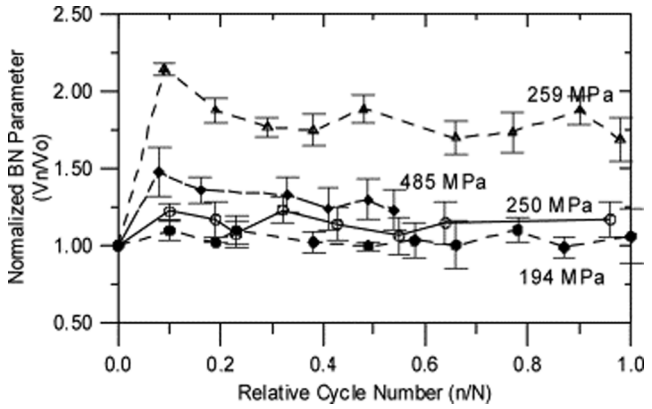

Fig. 13. Change of the normalized Barkhausen noise rms value in AISI 8620 steel specimens through the relative cycle number - axial machine (R = 0) [125]. (Reprinted from International Journal of Fatigue, Volume 27, Issue 6, E. S. Palma, T.R. Mansur, S. Ferreira Silva, A. Alvarenga, Fatigue damage assessment in AISI 8620 steel using Barkhausen noise, Pages 659–665, Copyright 2004, with permission from Elsevier.)

Sagar et al monitored the magnetic BHN peak voltage of a low carbon structural steel in [126], with the addition of microstructural analysis through transmission electron microscopy (TEM). They defined a three-stage process: (a) peak voltage increase due to the rearrangements and formation of dislocation cell structures, (b) a decrease in peak voltage, due to a reduction in cell size, increased dislocation density and formation of slip bands, and (c) an increase due to the initiation and growth of macro-cracks.

4.7.2. Hysteresis loops

In addition to the work performed in regard to BHN, researchers have also directly investigated the magnetic properties of materials. For example, Morishita et al. investigated the magnetic properties of A533B low alloy steel, under both plastic deformations and fatigue loading. They found that the residual magnetic flux density decreased continuously throughout the fatigue cycling. However, they also reported that there was no change in the coercive force throughout the investigation [127]. Gao et al. monitored the coercivity of the same type of steel, under the initial conditions of pre-strained and non-pre-strained, finding that they exhibited a reduction and increase in coercivity, respectively, in [128]. This might be due to the fact that Morishita's fatigue tests were performed with zero-tension cyclic load, and well within the high cycle fatigue (HCF) domain, whereas Gao's tests are very close to the LCF domain, with tension and compression fatigue tests. Gilanyi et al. found that the strongest property changes of the hysteresis loops related to fatigue damage were the remanent induction of the material [129]. Chen et al. performed a comparison of magnetic hysteresis and the magnetic Barkhausen effect in [130] for the same type of material. They concluded that the hysteresis parameters typically would not exhibit much change before the last 10–20% of the fatigue life, whereas the BHN signal amplitude would continuously decrease with the increasing number of loading cycles. Grimberg et al. investigated SAE 4130 under two different stress amplitudes and found, through the incremental magnetic permeability method, that the coercive force increased with an increasing number of fatigue cycles, reaching a level of about 595 A/m at failure for both load amplitudes. They concluded that the methodology could be used to predict the fatigue damage for SAE 4130 [131].

4.7.3. Deformation-induced phase transformation

Furthermore, it should be mentioned that there is also a magnetic method which exploits the deformation-induced phase transformation in austenitic stainless steels to martensite. In this regard, it is commonly the magnetic content in comparison to number of cycles which is used as damage parameter [132].

4.8. Ultrasonic methods

The commonly used ultrasonic methods for crack detection in materials are not sensitive enough to detect microstructural defects generated in the early stages of fatigue, as the defects are shorter than the wave length normally used in ultrasonics [133]. However, it has been shown by several researchers that parameters such as attenuation, velocity and secondary harmonics can be exploited to characterize the microstructural damage. These are commonly discussed as the nonlinear ultrasonic method and linear or attenuation and velocity methods.

4.8.1. Nonlinear ultrasonic method

The nonlinear ultrasonic method has its basis in the fact that, as an ultrasonic wave propagates through the nonlinear material, the signal will be distorted, and secondary harmonics will be developed. Thus, nonlinear behaviour is attributed to the microstructural nonlinearity of the propagation medium, which is commonly discussed in light of both microcracks and dislocations [134]. An example of this can be seen in Fig. 14 by Palit Sagar et al., who investigated in [5] the development of the secondary harmonic and compared it to the dislocation structure of different specimens of a low carbon structural steel, which had been fatigued to various percentages of the total fatigue life. Furthermore, the amplitude of the fundamental and secondary harmonic of the resulting

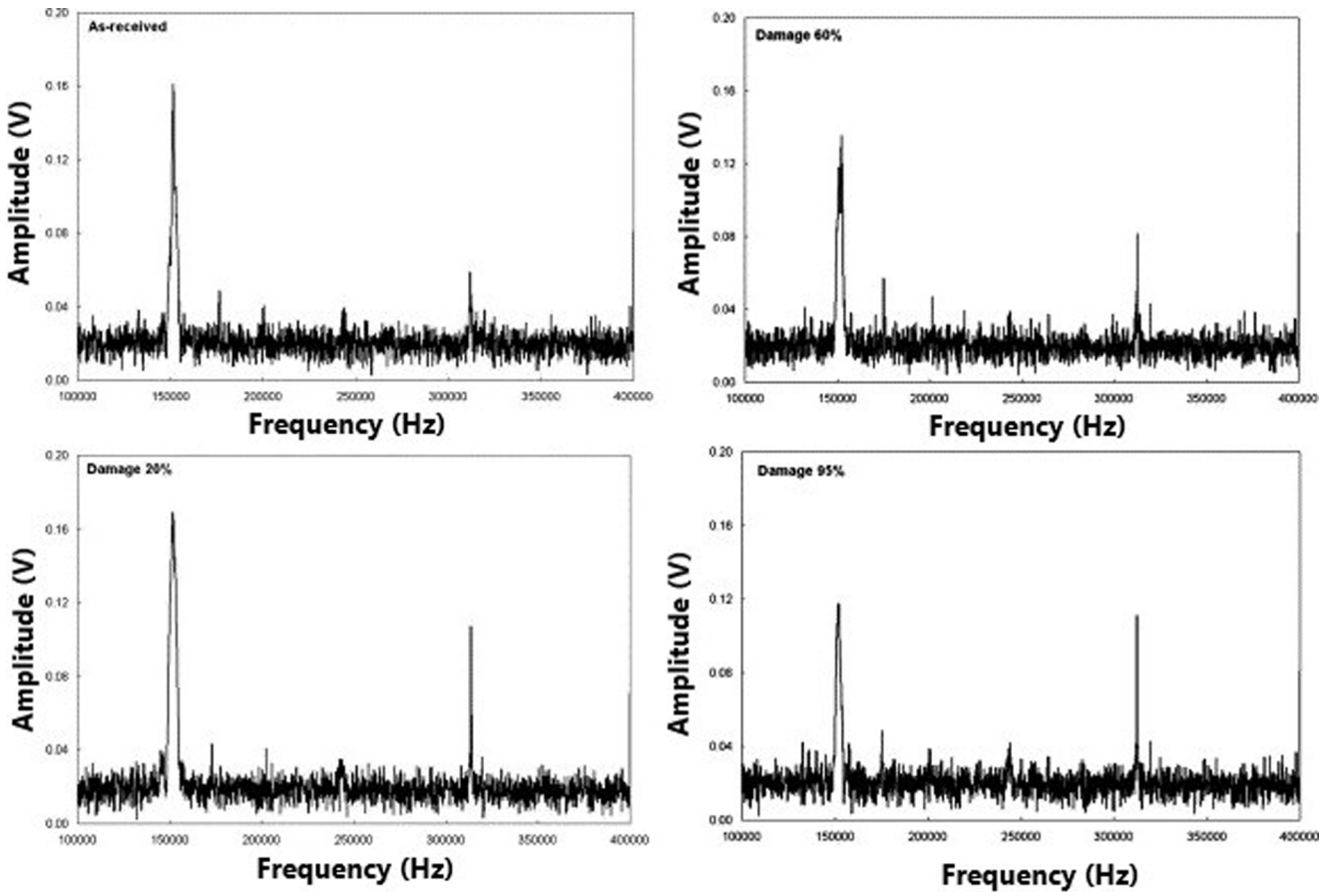

Fig. 14. Power spectrum of received signals during various stages of fatigue damage [5]. (Reprinted from Scripta Materialia, Volume 55, Issue 2, S. Palit Sagar, S. Das, N. Parida, D.K. Bhattacharya, Non-linear ultrasonic technique to assess fatigue damage in structural steel, Pages 199–202, Copyright 2006, with permission from Elsevier.)

power spectrum was compared in the form, total harmonic distortion (THD) given by $\%THD = \frac{A_2}{A_1}$, revealing a damage progression of first increasing, then plateauing, before further increasing. Cantrell and Yost investigated AA2024-T4 in [135] through the nonlinearity parameter β defined as $\beta \propto \frac{A_2}{A_1^2}$, A_1 and A_2 being the amplitude of the fundamental and second harmonic, respectively, revealing a monotonic increase with an increasing number of fatigue cycles. Kumar et al. investigated the possibility of in situ measurements during very high cycle fatigue (VHCF) damage accumulation in [136,137], by analysing the feedback signal of a closed-loop ultrasonic fatigue system. They highlighted the possibility of achieving additional information through ultrasonic fatigue testing, such as initial hardening/softening and crack initiation. Shui et al. discussed and demonstrated a method for and advantages of using low voltage generated Rayleigh waves, in the view of reducing instrumentation nonlinearity, being a single-sided, surface sensitive method which can be performed over large distances [138]. Jhang proposed a new method to measure β through bispectral analysis to remove noise, and investigated the nonlinear and linear parameters for mild steels (SS41 and SS45) in [139], revealing the proportionality of the nonlinear parameter with the applied load amplitude and the number of fatigue cycles. Furthermore, Jhang concluded that the velocity and attenuation did not exhibit any noticeable change. Nagy investigated both nonlinear and linear parameters for plastics, metals, composites and adhesives in [133], revealing the material dependence in metals on the evolution of the nonlinearity, and that the nonlinear parameter is fairly sensitive for all the aforementioned materials, whereas, in comparison, the linear parameters commonly exhibited small variation.

4.8.2. *Linear or attenuation and velocity methods*

It has been documented that a change also exists in the parameters of attenuation and velocity, although not as marked as in the nonlinear method. In [140], Ogi et al. investigated the attenuation and velocity change of 99 wt pct pure polycrystalline copper as a uniaxial stress state was applied, demonstrating that both longitudinal and shear waves are sensitive to dislocations, whereas the latter wave exhibits higher sensitivity. Ohtani et al. continuously monitored the change of attenuation and velocity in two annealed low carbon steels with 0.21 and 0.15 mass % C through the EMAR method in [141,142]. The experimental work also included TEM images and a discussion of the different stages observed. Both the investigated materials exhibited small regions of significant change and large regions with insignificant change. Liu et al. [143] measured the change in velocity and attenuation in nodular cast iron, finding that the attenuation parameter is a more pronounced parameter than speed for the specified material. Furthermore, through the graphs, it can be noted that this material, in contrast to the aforementioned material, exhibits a more continuous form, even though it exhibits a plateau for both parameters around half of the fatigue life. In [144], Yamagashi and Fukuhara monitored several mechanical parameters through the use of the ultrasonic shear wave and longitudinal wave velocities of extruded pure magnesium. However, the plots for the change of velocities are included in the paper, revealing a strong dependency on the domain of fatigue, as in if it is within the LCF, HCF or very high cycle fatigue (VHCF), consequently highlighting the stress/strain amplitude dependency. Kenderian et al. applied the Granato and Lücke [145,146] dislocation damping theory, to perform a relative estimation of the dislocation density and loop length in rail steel [147]. The study revealed a drastic change in the parameters within the first

10% of the fatigue life, before then showing a monotonic increasing or decreasing trend. Furthermore, a relaxation phenomenon due to paused cycling was discovered in regard to the parameter. The parameters would, however, quickly retrieve the previous value upon continued cycling.

5. Discussion

In light of the reviewed literature, two discussions and a section regarding comments on the way forward can be developed: one discussion from the perspective of general damage measurement and a second, focused on the case-dependent damage assessment.

5.1. General damage measurement

When it comes to the topic of applying a damage parameter to assess the accumulated damage through measurements, there are several considerations to be made.

It is evident that both the material in question and its initial dislocation structure will play a crucial part in the measurability of the accumulated damage and progression, respectively. In the review, it can be seen that methodology is material-dependent, for example in the case of positron annihilation. In fact, it was found that positron annihilation was not applicable for Al-2024, attributed to the initial presence of positron trapping sites, consequently masking the fatigue damage. Furthermore, it was noted that the initial dislocation structure will influence the parameter used for damage progression. This was seen in regard to both the X-ray diffraction and the hardness methodology, where the progression of the parameter in question would strongly depend on the initial dislocation structures resulting from as-machined/received, in contrast to annealed, specimens.

Applicability and measurability dependence, in regard to applied stress/strain with its accompanying stress/strain ratio and frequency, is an important factor to consider. In regard to the thermometric review, it was highlighted, for instance, that the dissipated energy in a unit volume per cycle has a stress/strain and ratio dependence, which could also be noted through the raise angle methodology for damage assessment. Furthermore, it can be seen that the reduction of the ultrasonic linear parameters exhibits vastly different degradation/damage curves for LCF, HCF and VHCF, consequently highlighting the damage progression dependence on the stress/strain range.

The desired region of the fatigue damage progression should be considered, as regards whether it is early or late in the fatigue life. Throughout the review, it is clear that most of the methodologies do not exhibit high measurability throughout the fatigue damage process, with the possible exception of X-ray diffraction with a carefully selected penetration depth. For instance, positron annihilation commonly exhibits the largest change early in the fatigue life, before then either converging or reaching saturation, resulting in a reduction or termination of measurability, respectively. However, methodologies such as electric resistance and strain-based methods seem to be more prominent in the late stages of fatigue, consequently resulting in different applicability. Positron annihilation could potentially be used in the early stages of fatigue, where the stresses are rather close to the knee-point stress amplitude, to signal whether or not damage has been introduced, whereas the electric resistance method will be more applicable towards the end of the fatigue life, although earlier than the initiation of a macroscopic crack.

Furthermore, the geometry in combination with the resulting local stress field has to be considered in light of the adapted measurement technique. This from the perspective that the measurement should preferably be performed in the same location to obtain comparable results, of the parameters change through cycling, or alternatively, in a location with similar stress gradients. For instance, when the hardness methodology is adapted, a measurement cannot be performed in the exact same location twice, consequently resulting in that a similar stress field should be measured. It should be noted that the measurement location and location of similar stress gradients also has to be the location or field of highest cyclic stress. Consequently, as it is commonly the location of crack initiation/failure.

The perspective of how the measurement itself is performed should also be considered, in regard to both whether the measurements have to be performed during operation and whether the measurement can be performed in situ. For instance, AE has the advantage of being focused on in-situ measurements, but these must be in the situation of a propagating crack, as in during operation, whereas the XRD and positron annihilation methods seem generally more applicable in laboratory experiments. However, the hardness, ultrasonic and magnetic parameters have the potential to be measured in situ.

5.2. Case-dependent damage assessment

The previous section ended with a short discussion regarding how the measurement itself is performed, as well as its applicability. In this section, methods are classified into three categories, based on the limitations of the applicability, as shown in Table 3. It is highlighted that the parameters applicable for in situ assessment can also be performed in a laboratory, and the parameters which can be laboratory assessment can also be good to develop a damage model. However, the table is simply constructed from the perspective of practical applications, not from that of accuracy, nor from the perspective of exhibiting continuity throughout the fatigue life. Furthermore, it can be noted that for damage assessment, access to the potentially damaged material is a requirement for the reviewed methods.

For damage assessment of structures in situ, the acoustic emission, hardness, ultrasonic, magnetic and potential drop methods were selected. This is from the perspective that portable equipment exists. The acoustic emission method would require to be monitored passively during loading of the component/structure, consequently meaning during operation. Furthermore, the hardness, ultrasonic, magnetic and potential drop methods do not depend on present cycling, meaning that the measurements can be performed when the component is at rest. However, if a nonzero nominal stress were present in the measured state, it should be accounted for. This is due to the fact that the four aforementioned methods are known to be influenced by the presence of stress/strain in the material. Furthermore, the electrical PDM method seems to be applicable within the category of in situ inspections, from the perspective of crack detection.

To the authors' knowledge, there is yet no commercially available portable equipment for positron annihilation and X-ray diffraction, feasible to perform in situ inspections. That said, there might be the potential for such equipment in the future. However, when it comes to the perspective of investigations of mechanical equipment, which can either be performed in a laboratory or even disassembled, their applications seem viable in the view of damage assessment.

The electrical resistance, strain and thermometric methods were not included for in situ or laboratory investigations. The thermometric methods were not included as it is a requirement to induce further damage to the component to evaluate the current damage state, consequently making it less attractive. Furthermore, the electrical resistance revealed that a large number of electrodes would be required to properly map the accumulated fatigue damage.

Table 3
Applicability of methods.

In situ assessment	Laboratory assessment	Damage model
Acoustic emission	Positron annihilation	Electric resistance
Hardness	X-ray diffraction	Strain-based
Ultrasonic		Thermometric
Magnetic		
Potential drop method		

Regarding laboratory experiments, from the perspective of better understanding and developing models for fatigue damage accumulation, all the different methods have their advantages and disadvantages as regards damage measurement, as highlighted in Section 5.1.

In addition, the various methods were categorized in regard to groups of materials, as can be seen in Table 4.

Furthermore, in Section 5.1, the topic of stress field and gradients were mentioned. This should also be considered regarding case-dependent damage assessment. This is from the perspective that notched specimens will commonly exhibit both stress concentrations, with high gradients, and a multiaxial stress state. Consequently, resulting in that the measurement techniques might not be comparable to the measured change under a uniaxial stress state. Furthermore, if it is assumed that there is an equivalent stress which will under the multiaxial cyclic stress be equivalent to the uniaxial cyclic stress, the measurement might still be challenging. This from the perspective that the measurement themselves might have to be performed over a variety of the stress contours, due to the area required to be measured, consequently not measuring one damage zone, but instead a vast number of damage zones. An example of this might be such as the hardness methodology, where an area has to be indented, regardless of which hardness testing method is applied. Consequently, resulting in that the indentation might cover a vast number of areas which have experienced different cyclic stress.

The topic of continuous measurements, or alternatively measurability during continuous operation should be considered. From the perspective of crack monitoring, the methods of potential drop method, acoustic emissions, and ultrasonics seems feasible. However, from the perspective of damage monitoring, the methods recommended for continuous monitoring is strain, thermometric, ultrasonic and magnetic.

6. Conclusions

The main conclusions and reflections regarding future work within the field of damage measurement are presented in this section. Additionally, the relevant key information and findings of reviewed fatigue damage detection and measurement techniques are clearly presented in Tables 5, 6 and 7.

Fatigue damage measurement through the discussed methods is commonly a rather time-consuming task. This is because each specimen has to be fatigue tested while also continuously being monitored, to achieve a single test result. Furthermore, it has been found that there are several test parameters which might affect the observed change throughout the fatigue life, as previously discussed, which further complicates the experimental work, subsequently resulting in the fact that exhaustive research is not necessarily an achievable task for a small research group alone. In light of this, it should be highlighted that extensive descriptions in experimental work will make the different work more comparable, which can result in better “knowledge gathering”. Some parameters considered as important to make the works more comparable can be found in Table 5, while a discussion on the various parameters is presented in Section 5.1.

Table 4
Applicability in regard to groups of material.

Metals	Composites
Potential drop method	Acoustic emissions
Electric resistance	X-ray diffraction
Acoustic emissions	Ultrasonic
Hardness-based	Strain-based
X-ray diffraction	Thermometric
Positron annihilation	
Magnetic	
Ultrasonic	
Thermometric	
Strain-based	

Table 5
Important information to document during damage measurement of fatigue.

Material	The material used – with material characteristics Surface finish and processing of the material Microstructure (especially if unknown material)	
Load parameters	Cyclic loading Stress amplitude R - Ratio Frequency Number of cycles	Spectrum loading Standard deviation Mean value Coefficient of variation of stress amplitude and R - Ratio
Measurement technique	Good explanation of the method used	
Criterion for fatigue failure	The criterion which is considered as fatigue failure should be highlighted, as in first crack, through thickness crack or final fracture	

Table 6
Summary of crack monitoring based on the reviewed literature.

Method	Parameter	Technique/ Phenomenon	Limitations	Discussion
Electric	$PDM = 1 - \frac{V_0}{V}$	Change in potential (voltage) field due to discontinuity in the material (Crack).	- From crack initiation. - Calibration curves must be developed.	The PDM method is well established in the monitoring of cracks via the calibration curves. However, such curves are geometry-dependent and must be developed for each case.
Acoustic emission	Amplitude; Counts; Duration; Energy; Risetime; Counts to Peak; Absolute Energy; Count rate $\log\left(\frac{dA}{dN}\right) = B\log(\Delta K) + \log(C)$	Elastic stress waves generated due to rapid release of energy from a localized source within a stressed material.	- Crack must be present. - Only measurable during propagation. - Signal processing/ interpretation. - Number of sensors defines accuracy, and the information that can be obtained.	Generally, for in situ monitoring of various structures, in contrast to laboratory/ specimen-scale testing. However, has a disadvantage in regard to unwanted noise and signal processing.
Ultrasonic method	Time of flight, Time of flight diffraction, energy, amplitude.	Elastic stress waves, commonly generated by the use of a piezoelectric crystal, with the resulting reflection or diffraction.	- Crack or loss of material must be present.	Common method to apply for in situ inspection of various components. TOFD seems most reliable for crack sizing, with the advantage of exhibiting good detectability as well.

As previously noted, some of the methodologies are more applicable from the perspective of obtaining additional information during common fatigue tests and, therefore, more applicable from the perspective of developing damage laws. However, for the methodologies where the

Table 7
Summary of damage monitoring based on the reviewed literature.

Method	Parameter	Technique/Phenomenon	Limitations	Discussion
Electric	Resistance $= \Delta R$; $\frac{\Delta R}{R}$; $R = \frac{\rho L}{A} \rightarrow \Delta\rho$	Increased resistivity due to dislocations, point defects, micro and macroscopic crack propagation.	- Conductive materials. - Most significant near fracture. - Small measurement ($\mu\Omega$). - Measurable outside operation.	Resistance seems more applicable to specimen testing, for additional information.
Hardness	Hv; Hb; $1 - \frac{H_D}{H_0}$; $H_D = C(1-D)k(\varepsilon + \varepsilon_H)^m$	Measurement of the surface hardening/softening due to cyclic microplasticity.	- Requires extensive polishing procedure before operation. - Requires microstructural analysis. - NDE perspective questionable. - Measurable outside operation.	Strong correlation with the fatigue damaging process. Disadvantage in regard to the polishing requirement. Furthermore, the method being non-destructive in view of fatigue is a subject for discussion.
X-ray diffraction	Halfwidth b; Integral width β; Fourier coefficients; Dislocation estimate $\bar{\rho} = \frac{\bar{\beta}^2}{9b^2}$	Broadening of the XRD peak due to micro stresses (dislocations) causing lattice distortion.	- Radiation penetration depth dictates the shape of the damage accumulation curve. - Measurable outside operation.	The penetration depth of the radiation used should be carefully considered. More towards laboratory testing in the literature.
Thermometric	ΔT; $\frac{\Delta T}{\Delta N}$; R_θ; $Q\left(\frac{kJ}{m^3 cycle}\right)$	Dissipation of heat energy due to internal friction (plastic deformation)	- Strongly stress- and frequency-dependent. - Has to be measured during operation/loading.	Strong relation to the accumulation of fatigue damage. Has limitations in practical applications. Consequently, cyclic loading must be applied to assess the damage. However, can easily be applied in parallel with fatigue testing, to obtain additional information.
Strain-based	Ratcheting: $\frac{\varepsilon_m - (\varepsilon_m)_{min}}{(\varepsilon_m)_{max} - (\varepsilon_m)_{min}}$ Inelastic strains: $\frac{\Delta\varepsilon^i - \Delta\varepsilon^i_0}{\Delta\varepsilon^i_f - \Delta\varepsilon^i_0}$	Ratcheting: Generated by the local deformation around voids, non-metallic precipitations and other defects within the material. Inelastic strains: Cyclic plasticity Both cases: Measurement of the cyclic nonlinear deformation	- Small measurement (magnitude around 10^{-4} or 10^{-3}) - Load must be applied to evaluate	Can give increased information in contrast to the thermometric method, as in if the fatigue is due to ratcheting or inelastic strains. However, smaller measurable values.
Positron annihilation	τ; S − parameter $=$ $\frac{\text{The counts of } \gamma - \text{ray near central peak}}{\text{Total counts of } \gamma - \text{ray}}$	Measurement of time from birth to annihilation and the energy of the resulting photons. Caused due to the development of vacancies through the fatigue loading.	- Measurability drops once the amount of positron trapping sites saturates (mainly measurable early in the fatigue life). - Not applicable for materials exhibiting saturation of positron trapping sites in initial state. - Mainly applicable in laboratories.	Applicability dependent on material characteristics. Due to the existence of initial positron traps such as, for instance, precipitates. The parameter is most significant early in the fatigue life. Might have the potential to monitor whether fatigue damage has accumulated or not, in either conservative designs with a high DFF or where "infinite" fatigue life is desired.
Magnetic	BHN: RMS (V); $\frac{V_n}{V_0}$ Magnetic hysteresis parameters	In both cases due to interaction of dislocation structures and the magnetic domain walls.	- Measurable without loading. - Only works for ferromagnetic materials or through stress-induced phase change. - Not applicable if yield has been surpassed. - Often large plateaus. - Measurable without loading.	Mainly for laboratory testing. The magnetic methods have a strong relation to the microstructure, as can be seen in the cited literature. However, in regard to monitoring fatigue damage, there are contradicting findings.
Ultrasonic	Nonlinear: $\beta \propto \frac{A_2}{A_1^2}$; $\%THD = \frac{A_2}{A_1} \times 100\%$ Linear: $\Delta V(\frac{m}{s})$; $\alpha(\mu s^{-1})$; $\frac{\Delta V}{V_0}$; $\frac{\Delta\alpha}{\alpha_0}$; $1 - \frac{V_L^2}{V_L^2}$; $1 \frac{-\alpha}{\alpha}$	Nonlinear: Attributed to the nonlinearity of the propagation medium, commonly discussed as microcracks and dislocations, generating secondary harmonics. Linear: Dislocation dampening.	- Linear methods exhibit small change often with large plateaus. - Measurable without loading.	The nonlinear method exhibits a continuous noticeable increase throughout the reviewed literature. The linear methods are generally more questionable, with large sections of insignificant change.

goal is to develop a diagnostic tool for the remaining fatigue life before a macroscopic crack has been initiated, it would be of importance to also consider factors such as bolted and welded joints, as fatigue failure is commonly associated with such details, due to the higher local stresses and often multiaxial fatigue in both categories, with the addition of mean stress/residual stresses, the presence of microcracks and the potential for unfavourable microstructure for welded details.

The methods are classified in the Table 3 based on the usage of laboratory and in-situ assessments. Table 4 categorized the applicability of the methods for metal and composites. Tables 6 and 7 summarized the parameters, phenomenon and limitations of all the crack monitoring and damage monitoring separately. The reliability, advantages, weaknesses and case dependency are presented at the last column of the tables. The important information such as material, load parameters, measurement technique and failure criterion, which should be investigated before monitoring, and relevant guidelines are presented in the Table 5. Therefore, these tables can be considered as a framework for choosing suitable technique for fatigue crack or damage detection of material or components and this is one of the main outcomes of the review paper.

Furthermore, validation of methods in regard to such as variable

amplitude loading (VAL) should be made. In the review, it was noted that both the thermometric and XRD method achieved reasonable accuracy for determining the remaining fatigue life during two and four stage block loadings. However, variable amplitude loadings and block loadings is not equivalent.

At last, it should be noted that even though microstructural changes throughout the fatigue life can be measured, it does not necessarily define the consumed nor remaining fatigue life. In fact, the only common practice to estimate remaining life through measurements, is by crack detection and crack propagation. Consequently, as it is the strongest and simplest indicator for fatigue damage. However, the continued research towards the field of damage measurement, through microstructural changes for the crack initiation phase, helps both in the understanding of fatigue mechanisms and developing damage accumulation rules. This from the perspective that the parameters adapted for damage measurements, are closely related to the microstructural progression of fatigue damage.

Declaration of Competing Interest

The authors declare that they have no known competing financial interests or personal relationships that could have appeared to influence the work reported in this paper.

Acknowledgement

The authors are grateful for the financial support provided by the Norwegian Ministry of Education during this project. Furthermore, the group wishes to thank the publishers for allowing the reuse of figures.

References

[1] DNVGL. RP-C203: Fatigue design of offshore steel structures; 2014.
[2] Keprate A, Ratnayake RMC. Fatigue and fracture degradation inspection of offshore structures and mechanical items: The state of the art. Proceedings of the International Conference on Offshore Mechanics and Arctic Engineering - OMAE. 2015.
[3] Wang QY, Berard JY, Rathery S, Bathias C. Technical note High-cycle fatigue crack initiation and propagation behaviour of high-strength sprin steel wires. Fatigue Fract Eng Mater Struct 1999;22(8):673–7.
[4] Suresh S. Fatigue of materials. 1st paperback ed. (with corrections and exercises). Cambridge solid state science series, vol. 8. Cambridge: Cambridge University Press; 1992.
[5] Palit Sagar S, Das S, Parida N, Bhattacharya DK. Non-linear ultrasonic technique to assess fatigue damage in structural steel. Scr Mater 2006;55(2):199–202.
[6] Lukáš P, Kunz L. Specific features of high-cycle and ultra-high-cycle fatigue. Fatigue Fract Eng Mater Struct 2002;25(8–9):747–53.
[7] Pippan R, Zelger C, Gach E, Bichler C, Weinhandl H. On the mechanism of fatigue crack propagation in ductile metallic materials. Fatigue Fract Eng Mater Struct 2011;34(1):1–16.
[8] Yang L, Fatemi A. Cumulative fatigue damage mechanisms and quantifying parameters: A literature review. J Test Eval 1998;26(2):89–100.
[9] Ritchie RO, Garrett GG, Knott JP. Crack-growth monitoring: Optimisation of the electrical potential technique using an analogue method. Int J FractMech 1971;7 (4):462.
[10] Tada N. Application of direct-current potential difference method to evaluation of various damages in conductive materials. American Society of Mechanical Engineers, Pressure Vessels and Piping Division (Publication) PVP. 2008.
[11] Gandossi L, Summers SA, Taylor NG, Hurst RC, Hulm BJ, Parker JD. The potential drop method for monitoring crack growth in real components subjected to combined fatigue and creep conditions: Application of FE techniques for deriving calibration curves. Int J Press Vessels Pip 2001;78(11–12):881–91.
[12] Spitas V, Spitas C, Michelis P. A three-point electrical potential difference method for in situ monitoring of propagating mixed-mode cracks at high temperature. Meas J Int Meas Confeder 2010;43(7):950–9.
[13] Tada N, Hayashi Y, Kitamura T, Ohtani R. Analysis on the applicability of direct current electrical potential method to the detection of damage by multiple small internal cracks. Int J Fract 1997;85(1):1–9.
[14] Sonsino CM. Comparison of different local design concepts for the structural durability assessment of welded offshore K-nodes. Int J Fatigue 2012;34(1): 27–34.
[15] Černý I. The use of DCPD method for measurement of growth of cracks in large components at normal and elevated temperatures. Eng Fract Mech 2004;71(4): 837–48.
[16] Oppermann W, Hofstötter P, Keller HP. Long-term installations of the DC-potential drop method in four nuclear power plants and the accuracies thereby obtained for monitoring of crack initiation and crack growth 1 This paper was presented at the 21st MPA Seminar, Stuttgart, 5th–6th October 1995.1. Nucl Eng Des 1997;174(3): 287–92.
[17] Roberts TM, Talebzadeh M. Acoustic emission monitoring of fatigue crack propagation. J Constr Steel Res 2003;59(6):695–712.
[18] Anastasopoulos A, Kourousis D, Botten S, Wang G. Acoustic emission monitoring for detecting structural defects in vessels and offshore structures. Ships Offshore Struct 2009;4(4):363–72.
[19] Yu J, Ziehl P, Matta F, Pollock A. Acoustic emission detection of fatigue damage in cruciform welded joints. J Constr Steel Res 2013;86:85–91.
[20] Mazur K, Wisner B, Kontsos A. Fatigue damage assessment leveraging nondestructive evaluation data. JOM 2018;70(7):1182–9.
[21] Sedlak P, Hirose Y, Enoki M. Acoustic emission localization in thin multi-layer plates using first-arrival determination. Mech Syst Sig Process 2013;36(2): 636–49.
[22] Bai F, Gagar D, Foote P, Zhao Y. Comparison of alternatives to amplitude thresholding for onset detection of acoustic emission signals. Mech Syst Sig Process 2017;84:717–30.
[23] Tang J, Soua S, Mares C, Gan TH. An experimental study of acoustic emission methodology for in service condition monitoring of wind turbine blades. Renew Energy 2016;99:170–9.
[24] Berkovits A, Fang D. Study of fatigue crack characteristics by acoustic emission. Eng Fract Mech 1995;51(3). 401–9, 411–6.
[25] Roberts TM, Talebzadeh M. Fatigue life prediction based on crack propagation and acoustic emission count rates. J Constr Steel Res 2003;59(6):679–94.
[26] Yu J, Ziehl P, Zrate B, Caicedo J. Prediction of fatigue crack growth in steel bridge components using acoustic emission. J Constr Steel Res 2011;67(8):1254–60.
[27] Keshtgar A, Modarres M. Acoustic emission-based fatigue crack growth prediction. Proceedings - Annual Reliability and Maintainability Symposium. 2013.
[28] Yuyama S, Yokoyama K, Niitani K, Ohtsu M, Uomoto T. Detection and evaluation of failures in high-strength tendon of prestressed concrete bridges by acoustic emission. Constr Build Mater 2007;21(3):491–500.
[29] Nair A, Cai CS. Acoustic emission monitoring of bridges: Review and case studies. Eng Struct 2010;32(6):1704–14.
[30] Yu L, Momeni S, Godinez V, Giurgiutiu V, Ziehl P, Yu J. Dual mode sensing with low-profile piezoelectric thin wafer sensors for steel bridge crack detection and diagnosis. Adv Civ Eng 2012;2012.
[31] Bruzelius K, Mba D. An initial investigation on the potential applicability of Acoustic Emission to rail track fault detection. NDT E Int 2004;37(7):507–16.
[32] Kuang KSC, Li D, Koh CG. Acoustic emission source location and noise cancellation for crack detection in rail head. Smart Struct Syst 2016;18(5): 1063–85.
[33] van der Horst MP, Kaminski ML, Puik E. Methods for Sensing and Monitoring Fatigue Cracks and Their Applicability for Marine Structures; 2013.
[34] Manjula K, Vijayarekh K, Venkatrama B. Weld Flaw Detection Using Various Ultrasonic Techniques: A Review. J Appl Sci 2014;14:1529–35.
[35] Baskaran G, Balasubramaniam K, Lakshmana Rao C. Shear-wave time of flight diffraction (S-TOFD) technique. NDT E Int 2006;39(6):458–67.
[36] Felice MV, Fan Z. Sizing of flaws using ultrasonic bulk wave testing: A review. Ultrasonics 2018;88:26–42.
[37] Moles M, Robertson LB, Sinclair T. Developments in Time-Of-Flight Diffraction (TOFD); 2012.
[38] Nath SK, Balasubramaniam K, Krishnamurthy CV, Narayana BH. Sizing of surface-breaking cracks in complex geometry components by ultrasonic Time-of-Flight Diffraction (TOFD) technique. Insight: Non-Destruct Test Cond Monit 2007;49(4):200–6.
[39] Nath SK, Balasubramaniam K, Krishnamurthy CV, Narayana BH. Reliability assessment of manual ultrasonic time of flight diffraction (TOFD) inspection for complex geometry components. NDT E Int 2010;43(2):152–62.
[40] Habibpour-Ledari A, Honarvar F. Three Dimensional Characterization of Defects by Ultrasonic Time-of-Flight Diffraction (ToFD) Technique. J Nondestr Eval 2018; 37(1):14.
[41] Young-Fo C, Cheng IH. Time of flight diffraction imaging for double-probe technique. IEEE Trans Ultrason Ferroelectr Freq Control 2002;49(6):776–83.
[42] Baskaran G, Balasubramaniam K, Krishnamurthy CV, Rao CL. Ultrasonic TOFD flaw sizing and imaging in thin plates using embedded signal identification technique (ESIT). Insight: Non-Destruct Test Cond Monit 2004;46(9):537–42.
[43] Subbaratnam R, Abraham ST, Venkatraman B, Raj B. Immersion and TOFD (I-TOFD): A Novel Combination for Examination of Lower Thicknesses. J Nondestr Eval 2011;30(3):137.
[44] Masserey B, Fromme P. In-situ monitoring of fatigue crack growth using high frequency guided waves. NDT E Int 2015;71:1–7.
[45] Grubisic V, Sonsino CM. Fatigue strength of high-pressure vessels for novel manufacturing processes. Fraunhofer Inst. for Structural Durability LBF, Report No. 148; 1979.
[46] Polák J. Electrical resistivity of cyclically deformed copper. Czech J Phys 1969;19 (3):315–22.
[47] Sun B, Guo Y. High-cycle fatigue damage measurement based on electrical resistance change considering variable electrical resistivity and uneven damage. Int J Fatigue 2004;26(5):457–62.
[48] Starke P, Eifler D, Boller C. Fatigue assessment of metallic materials beyond strain measurement. Int J Fatigue 2016;82:274–9.
[49] Germann H, Starke P, Eifler D. Resistivity-based evaluation of the fatigue behavior of cast irons. Metall Mater Trans A 2012;43(8):2792–8.

[50] Mao H, Yi X, Mao H, Tang W, Huang Z, Li X, et al. Fatigue damage detection and location of metal materials by electrical impedance tomography. Res Phys 2019;15.

[51] Klein M, Eifler D. Influences of the manufacturing processes on the surface integrity and the resulting fatigue behavior of quenched and tempered SAE 4140. Procedia Eng 2010.

[52] Sun B, Yang L, Guo Y. A high-cycle fatigue accumulation model based on electrical resistance for structural steels. Fatigue Fract Eng Mater Struct 2007;30(11):1052–62.

[53] Balle F, Huxhold S, Wagner G, Eifler D. Damage monitoring of ultrasonically welded aluminum/CFRP-joints by electrical resistance measurements. Procedia Eng 2011.

[54] Walther F, Eifler D. Cyclic deformation behavior of steels and light-metal alloys. Mater Sci Eng, A 2007;468–470(SPEC. ISS.):259–66.

[55] Starke P, Klein M, Eifler D. Resistivity - A characteristic fingerprint of fatigue induced changes in the microstructure of metallic materials. Procedia Eng 2011.

[56] Walther F, Eifler D. Fatigue life calculation of SAE 1050 and SAE 1065 steel under random loading. Int J Fatigue 2007;29(9–11):1885–92.

[57] Kucharczyk P, Rizos A, Münstermann S, Bleck W. Estimation of the endurance fatigue limit for structural steel in load increasing tests at low temperature. Fatigue Fract Eng Mater Struct 2012;35(7):628–37.

[58] Pavlou DG, Prediction of Fatigue Damage Accumulation under Real Loading Spectra. University of Patras; 1994.

[59] Pavlou DG. A phenomenological fatigue damage accumulation rule based on hardness increasing, for the 2024–T42 aluminum. Eng Struct 2002;24(11):1363–8.

[60] Ye DY, Wang DJ, An P. Characteristics of the change in the surface microhardness during high cycle fatigue damage. Mater Chem Phys 1996;44(2):179–81.

[61] Ye D, Tong X, Yao L, Yin X. Fatigue hardening/softening behaviour investigated through Vickers microhardness measurement during high-cycle fatigue. Mater Chem Phys 1998;56(3):199–204.

[62] Ye D, Wang Z. Approach to investigate pre-nucleation fatigue damage of cyclically loaded metals using Vickers microhardness tests. Int J Fatigue 2001;23(1):85–91.

[63] Drumond G, Pinheiro B, Pasqualino I, Roudet F, Chicot D, Decoopman X. High Cycle Fatigue Damage Evaluation of Steel Pipelines Based on Microhardness Changes During Cyclic Loads. ASME 2017 36th International Conference on Ocean, Offshore and Arctic Engineering. 2017.

[64] Drumond G, Pinheiro B, Pasqualino I, Roudet F, Chicot D. High Cycle Fatigue Damage Evaluation of Steel Pipelines Based on Microhardness Changes During Cyclic Loads: Part II. ASME 2018 37th International Conference on Ocean, Offshore and Arctic Engineering. 2018.

[65] Drumond G, Roudet F, Chicot D, Pinheiro B, Pasqualino I. A damage criterion to predict the fatigue life of steel pipelines based on indentation measurements. J Offshore Mech Arct Eng 2021;143(1).

[66] Miroslav Š, Vladimír C, Kepka M. Possibility of fatigue damage detection by non-destructive measurement of the surface hardness. Procedia Structural Integrity. 2017.

[67] Pinheiro B, Lesage J, Pasqualino I, Benseddiq N, Bemporad E. X-ray diffraction study of microstructural changes during fatigue damage initiation in steel pipes. Mater Sci Eng, A 2012;532:158–66.

[68] Vijayan K, Mani A, Balasingh C, Singh AK. X-ray analysis of polycrystalline aluminium subjected to fatigue cycling. Bull Mater Sci 1988;10(3):205–16.

[69] Nagao M, Weiss V. X-ray diffaction study of low cycle fatigue damage in plain carbon steel. American Society of Mechanical Engineers (Paper); 1976(76 -WA/Mat-10).

[70] Pangborn RN, Weissmann S, Kramer IR. Dislocation distribution and prediction of fatigue damage. Metall Trans A 1981;12(1):109–20.

[71] Kramer IR, Feng CR, Wu B. Dislocation-depth distribution in fatigued metals. Mater Sci Eng 1986;80(1):37–48.

[72] Pinheiro B, Lesage J, Pasqualino I, Bemporad E, Benseddiq N. X-ray diffraction study of microstructural changes during fatigue damage initiation in pipe steels: Role of the initial dislocation structure. Mater Sci Eng, A 2013;580:1–12.

[73] Teng Z, Wu H, Boller C, Starke P. A unified fatigue life calculation based on intrinsic thermal dissipation and microplasticity evolution. Int J Fatigue 2020;131.

[74] Harig H, Weber M. Estimation of crack initiation in plain carbon steels by thermometric methods. In: Sih GC, Provan JW, editors. Defects, Fracture and Fatigue. Dordrecht: Springer; 1983.

[75] Wang H, Jiang L, Liaw PK, Brooks CR, Klarstrom DL. Infrared temperature mapping of ULTIMET alloy during high-cycle fatigue tests. Metall Mater Trans A 2000;31(4):1307–10.

[76] Wagner D, Ranc N, Bathias C, Paris PC. Fatigue crack initiation detection by an infrared thermography method. Fatigue Fract Eng Mater Struct 2010;33(1):12–21.

[77] La Rosa G, Risitano A. Thermographic methodology for rapid determination of the fatigue limit of materials and mechanical components. Int J Fatigue 2000;22(1):65–73.

[78] Curà F, Curti G, Sesana R. A new iteration method for the thermographic determination of fatigue limit in steels. Int J Fatigue 2005;27(4):453–9.

[79] Luong MP. Infrared thermographic scanning of fatigue in metals. Nucl Eng Des 1995;158(2–3):363–76.

[80] Luong MP. Fatigue limit evaluation of metals using an infrared thermographic technique. Mech Mater 1998;28(1–4):155–63.

[81] Risitano A, Risitano G. Determining fatigue limits with thermal analysis of static traction tests. Fatigue Fract Eng Mater Struct 2013;36(7):631–9.

[82] Teng Z, Wu H, Boller C, Starke P. Thermography in high cycle fatigue short-term evaluation procedures applied to a medium carbon steel. Fatigue Fract Eng Mater Struct 2020;43(3):515–26.

[83] Fargione G, Geraci A, La Rosa G, Risitano A. Rapid determination of the fatigue curve by the thermographic method. Int J Fatigue 2002;24(1):11–9.

[84] Amiri M, Khonsari MM. Rapid determination of fatigue failure based on temperature evolution: Fully reversed bending load. Int J Fatigue 2010;32(2):382–9.

[85] Wu H, Bäumchen A, Engel A, Acosta R, Boller C, Starke P. SteBLife – A new short-time procedure for the evaluation of fatigue data. Int J Fatigue 2019;124:82–8.

[86] Starke P. StressLifetc – NDT-related assessment of the fatigue life of metallic materials. Materialpruefung/Mater Test 2019;61(4):297–303.

[87] Sonsino CM. Course of SN-curves especially in the high-cycle fatigue regime with regard to component design and safety. Int J Fatigue 2007;29(12):2246–58.

[88] Newman JC. Fatigue and Crack-growth Analyses under Giga-cycle Loading on Aluminum Alloys. Procedia Eng 2015;101:339–46.

[89] Meneghetti G. Analysis of the fatigue strength of a stainless steel based on the energy dissipation. Int J Fatigue 2007;29(1):81–94.

[90] Boulanger T, Chrysochoos A, Mabru C, Galtier A. Calorimetric analysis of dissipative and thermoelastic effects associated with the fatigue behavior of steels. Int J Fatigue 2004;26(3):221–9.

[91] Liaw PK, Wang H, Jiang L, Yang B, Huang JY, Kuo RC, et al. Thermographic detection of fatigue damage of pressure vessel steels at 1,000 Hz and 20 Hz. Scr Mater 2000;42(4):389–95.

[92] Amiri M, Khonsari MM. Nondestructive estimation of remaining fatigue life: Thermography technique. J Fail Anal Prev 2012;12(6):683–8.

[93] Liakat M, Khonsari MM. An experimental approach to estimate damage and remaining life of metals under uniaxial fatigue loading. Mater Des 2014;57:289–97.

[94] Dietrich L, Radziejewska J. The fatigue damage development in a cast Al-Si-Cu alloy. Mater Des 2011;32(1):322–9.

[95] Moćko W, Grzywna P, Kowalewski ZL, Radziejewska J. An influence of cyclic loading on the form of constitutive relationship for DP500 steel. Mater Des 2016;103:183–93.

[96] Moćko W. The influence of stress-controlled tensile fatigue loading on the stress-strain characteristics of AISI 1045 steel. Mater Des 2014;58:145–53.

[97] Socha G. Experimental investigations of fatigue cracks nucleation, growth and coalescence in structural steel. Int J Fatigue 2003;25(2):139–47.

[98] Socha G. Prediction of the fatigue life on the basis of damage progress rate curves. Int J Fatigue 2004;26(4):339–47.

[99] Sonsino CM. The influence of coldforming on the low cycle fatigue behaviour of the finegrained structural steel Fe E 47 and the age-hardened aluminium alloy AlCuMg2. Int J Fatigue 1984;6(3):173–83.

[100] Dupasquier A, Kögel G, Somoza A. Studies of light alloys by positron annihilation techniques. Acta Mater 2004;52(16):4707–26.

[101] Čížek J. Characterization of lattice defects in metallic materials by positron annihilation spectroscopy: A review. J Mater Sci Technol 2018;34(4):577–98.

[102] Puska MJ, Nieminen RM. Theory of positrons in solids and on solid surfaces. Rev Mod Phys 1994;66(3):841–97.

[103] Holzwarth U, Schaaff P. Nondestructive monitoring of fatigue damage evolution in austenitic stainless steel by positron-lifetime measurements. Phys Rev B Condens Matter Mater Phys 2004;69(9).

[104] Nagoshi T, Kozu S, Inoue Y, O'Rourke BE, Harada Y. Fatigue damage assessment of SUS316L using EBSD and PALS measurements. Mater Charact 2019;154:61–6.

[105] Uematsu Y, Kakiuchi T, Hattori K, Uesugi N, Nakao F. Non-destructive evaluation of fatigue damage and fatigue crack initiation in type 316 stainless steel by positron annihilation line-shape and lifetime analyses. Fatigue Fract Eng Mater Struct 2017;40(7):1143–53.

[106] Kawaguchi Y, Nakamura N, Yusa S. Non-destructive evaluation of fatigue damage in type 316 stainless steel using positron annihilation lineshape analysis. Mater Trans 2002;43(4):727–34.

[107] Kawaguchi Y, Shirai Y. Fatigue evaluation of type 316 stainless steel using positron annihilation lineshape analysis and $\beta+$-γ coincidence positron lifetime measurement. J Nucl Sci Technol 2002;39(10):1033–40.

[108] Maeda N, Nakamura N, Uchida M, Ohta Y, Yoshida K. Application of positron annihilation line-shape analysis to fatigue damage for nuclear plant materials. Nucl Eng Des 1996;167(2):169–74.

[109] Asoka-Kumar P, Hartley JH, Howell RH, Sterne PA, Akers D, Shah V, et al. Direct observation of carbon-decorated defects in fatigued type 304 stainless steel using positron annihilation spectroscopy. Acta Mater 2002;50(7):1761–70.

[110] Hori F, Oshima R. Positron annihilation study in the early stage of fatigue in type 304 stainless steel. Phys Status Solidi (A) Appl Res 2002;191(2):409–17.

[111] Holzwarth U, Schaaff P. On the non-destructive detection of fatigue damage in industrial aluminium alloys by positron annihilation. J Mater Sci 2007;42(14):5620–8.

[112] Tomáš I, Kovářík O, Kadlecová J, Vértesy G. Optimization of fatigue damage indication in ferromagnetic low carbon steel. Meas Sci Technol 2015;26(9).

[113] Kikuchi H, Ara K, Kamada Y, Kobayashi S. Effect of microstructure changes on Barkhausen noise properties and hysteresis loop in cold rolled low carbon steel. IEEE Trans Magn 2009;45(6):2744–7.

[114] Kasai N, Koshino H, Sekine K, Kihira H, Takahashi M. Study on the effect of elastic stress and microstructure of low carbon steels on Barkhausen noise. J Nondestr Eval 2013;32(3):277–85.

[115] Teschke M, Vasquez JR, Lücker L, Walther F. Characterization of damage evolution on hot flat rolled mild steel sheets by means of micromagnetic parameters and fatigue strength determination. Materials 2020;13(11).

[116] Yamaura S, Furuya Y, Watanabe T. The effect of grain boundary microstructure on Barkhausen noise in ferromagnetic materials. Acta Mater 2001;49(15):3019–27.
[117] Dijkstra LJ, Wert C. Effect of inclusions on coercive force of iron. Phys Rev 1950;79(6):979–85.
[118] Astie B, Degauque J. Influence of the dislocation structures on the magnetic and magnetomechanical properties of high-purity iron. IEEE Trans Magn 1981;17(6):2929–31.
[119] Scherpereel DE, Kazmerski LL, Allen CW. The magnetoelastic interaction of dislocations and ferromagnetic domain walls in iron and nickel. Metall Mater Trans B 1970;1(2):517–24.
[120] Deng Y, Li Z, Chen J, Qi X. The effects of the structure characteristics on Magnetic Barkhausen noise in commercial steels. J Magn Magn Mater 2018;451:276–82.
[121] Baldev R, Jayakumar T, Moorthy V, Vaidyanathan S. Characterisation of microstructures, deformation, and fatigue damage in different steels using magnetic Barkhausen emission technique. Russ J Nondestr Test 2001;37(11):789–98.
[122] Lindgren M, Lepistö T. Application of a novel type Barkhausen noise sensor to continuous fatigue monitoring. NDT E Int 2000;33(6):423–8.
[123] Lindgren M, Lepistö T. Effect of cyclic deformation on Barkhausen noise in a mild steel. NDT E Int 2003;36(6):401–9.
[124] Soultan M, Kleber X, Chicois J, Vincent A. Mechanical Barkhausen noise during fatigue of iron. NDT E Int 2006;39(6):493–8.
[125] Palma ES, Mansur TR, Silva Jr SF, Alvarenga Jr A. Fatigue damage assessment in AISI 8620 steel using Barkhausen noise. Int J Fatigue 2005;27(6):659–65.
[126] Sagar SP, Parida N, Das S, Dobmann G, Bhattacharya DK. Magnetic Barkhausen emission to evaluate fatigue damage in a low carbon structural steel. Int J Fatigue 2005;27(3):317–22.
[127] Morishita K, Gilanyi A, Sukegawa T, Uesaka T, Miya K. Magnetic non-destructive evaluation of accumulated fatigue damage in ferromagnetic steels for nuclear plant component. J Nucl Mater 1998;258–263(PART 2 B):1946–52.
[128] Gao Z, Chen ZJ, Jiles DC, Biner S. Variation of coercivity of ferromagnetic material during cyclic stressing. IEEE Trans Magn 1994;30(6):4593–5.
[129] Gilanyi A, Morishita K, Sukegawa T, Uesaka M, Miya K. Magnetic nondestructive evaluation of fatigue damage of ferromagnetic steels for nuclear fusion energy systems. Fusion Eng Des 1998;42(1–4):485–91.
[130] Chen ZJ, Strom A, Jiles DC. Micromagnetic surface measurements for evaluation of surface modifications due to cyclic stress. IEEE Trans Magn 1993;29(6):3031–3.
[131] Grimberg R, Leitoiu S, Bradu BE, Savin A, Andreescu A. Magnetic sensor used for the determination of fatigue state in ferromagnetic steels. Sens Actuators, A 2000;81(1):371–3.
[132] De Backer F, Schoss V, Maussner G. Investigations on the evaluation of the residual fatigue life-time in austenitic stainless steels. Nucl Eng Des 2001;206(2–3):201–19.
[133] Nagy PB. Fatigue damage assessment by nonlinear ultrasonic materials characterization. Ultrasonics 1998;36(1–5):375–81.
[134] Oruganti RK, Sivaramanivas R, Karthik TN, Kommareddy V, Ramadurai B, Ganesan B, et al. Quantification of fatigue damage accumulation using non-linear ultrasound measurements. Int J Fatigue 2007;29(9–11):2032–9.
[135] Cantrell JH, Yost WT. Nonlinear ultrasonic characterization of fatigue microstructures. Int J Fatigue 2001;23(SUPPL. 1):487–90.
[136] Kumar A, Adharapurapu RR, Jones JW, Pollock TM. In situ damage assessment in a cast magnesium alloy during very high cycle fatigue. Scr Mater 2011;64(1):65–8.
[137] Kumar A, Torbet CJ, Pollock TM, Wayne Jones J. In situ characterization of fatigue damage evolution in a cast Al alloy via nonlinear ultrasonic measurements. Acta Mater 2010;58(6):2143–54.
[138] Shui G, Kim JY, Qu J, Wang YS, Jacobs LJ. A new technique for measuring the acoustic nonlinearity of materials using Rayleigh waves. NDT E Int 2008;41(5):326–9.
[139] Jhang KY. Applications of nonlinear ultrasonics to the NDE of material degradation. IEEE Trans Ultrason Ferroelectr Freq Control 2000;47(3):540–8.
[140] Ogi H, Suzuki N, Hirao M. Noncontact ultrasonic spectroscopy on deforming polycrystalline copper: Dislocation damping and acoustoelasticity. Metall Mater Trans A 1998;29(12):2987–93.
[141] Ohtani T, Nishiyama K, Yoshikawa S, Ogi H, Hirao M. Ultrasonic attenuation and microstructural evolution throughout tension-compression fatigue of a low-carbon steel. Mater Sci Eng, A 2006;442(1–2 SPEC. ISS.):466–70.
[142] Ohtani T, Ogi H, Minami Y, Hirao M. Ultrasonic attenuation monitoring of fatigue damage in low carbon steels with electromagnetic acoustic resonance (EMAR). J Alloy Compd 2000;310(1–2):440–4.
[143] Liu JH, Li GL, Hao XY, Zeng DB, Sun ZH. Ultrasonic measurement of fatigue damage of nodular cast iron. Mater Lett 2001;50(4):194–8.
[144] Yamagishi H, Fukuhara M. Degradation behavior of moduli in extruded pure magnesium during low- to giga-scale cyclic tension fatigue. Acta Mater 2012;60(12):4759–67.
[145] Granato A, Lücke K. Theory of mechanical damping due to dislocations. J Appl Phys 1956;27(6):583–93.
[146] Granato A, Lücke K. Application of dislocation theory to internal friction phenomena at high frequencies. J Appl Phys 1956;27(7):789–805.
[147] Kenderian S, Berndt TP, Green Jr RE, Djordjevic BB. Ultrasonic monitoring of dislocations during fatigue of pearlitic rail steel. Mater Sci Eng, A 2003;348(1–2):90–9.